Late Pleistocene large-bodied mammalian fauna from Mocun cave in south China: Palaeontological, chronological and biogeographical implications

Yaobin Fan, Qingfeng Shao, Anne-Marie Bacon, Wei Liao, Wei Wang

Late Pleistocene large-bodied mammalian fauna from Mocun cave in south China: Palaeontological, chronological and biogeographical implications

Yaobin Fan[a], Qingfeng Shao[b], Anne-Marie Bacon[c], Wei Liao[a*], Wei Wang[a*]

a Institute of Culture Heritage, Shandong University, Qingdao, 266237, China
b School of Geography, Nanjing Normal University, Nanjing, 210023, China
c *Université Paris Cité, CNRS, BABEL, 75012 Paris, France*

Abstract: This paper reports the discovery of a new mammalian assemblage at Mocun cave in 2000 by the Natural History Museum of Guangxi. The Mocun site is located in a residual karst peak in southwest Guangxi, south China. Abundant mammalian fossil teeth and bones were extracted from relatively thick deposits, well constrained stratigraphically. The results show that 1) the Mocun fauna is composed of typical species of the "*Ailuropoda-Stegodon* association", including *Stegodon, Ailuropoda, Rhinoceros, Pongo, Tapirus*, *Megatapirus,* and *Elephas,* common in the Middle to the Late Pleistocene, with a larger portion of modern species; 2) By employing U-series dating (MC-ICP-MS) method on both the soda straw stalactites and mammalian teeth collected from deposits, the age of the Mocun fauna has been constrained between 66 and 101 ka, a transitional period from the interglacial stage MIS5 to the beginning of the last glacial stage (MIS4), representing one of the securely dated Late Pleistocene sites in southern China so far; 3) The composition in large mammals suggests a forested environment which harboured a great biodiversity in large species; 4) The taphonomic analysis indicates that the fossil accumulation is mainly due to activities of porcupines and to water flows; 5) Interestingly, our taxonomic study reveals some changes in the occurrence of *Tapirus sinensis* and *Megatapirus augustus* between ~66 and ~86 Ka, along with a change in the abundance of artiodactyls *versus* primates. It remains to demonstrate with more comprehensive records if these changes may be related to the mid-Late Pleistocene climatic transition.

Keywords: Southeast Asia, Karstic landscape, Regional evolution, U-series dating, "*Ailuropoda-Stegodon*" fauna

*Corresponding authors.
E-mail addresses: liaowei@sdu.edu.cn (W. Liao), wangw@sdu.edu.cn (W. Wang)

1. Introduction

During the Pleistocene, the "*Ailuropoda-Stegodon*" fauna (*sensu lato*) was a typical fauna of large-bodied mammals widely distributed from East Asia to mainland Southeast Asia (e. g. Colbert, 1943; Patte, 1928; Fromaget, 1936; de Terra, 1938; Beden and Guerin, 1973; Pope et al., 1981). In the Early Pleistocene, its range expanded north to the Qinling Mountains, the geographical boundary between north and south China, and its northern more limit reached the Lantian site in Shaanxi province, dated to 1.3 Million years ago [Ma], at the latitude 34°N (Hu and Qi, 1978; Qiu, 2006). In the Middle Pleistocene, the southern more limit is documented by the Thum Wiman Nakin site in Thailand, >169 000 years ago [ka], at the latitude 15.8°N (Tougard, 2001; Esposito et al., 2002; Suraprasit et al., 2020). The distribution range of the "*Ailuropoda-Stegodon*" fauna in China coincides with areas of subtropical monsoon climate.

The study of Pleistocene mammalian assemblages from southern China dates back to the beginning of the last century (Matthew and Granger, 1923; Young, 1929; Pei, 1935). Thereafter, since the middle of the century, as fossil sites were discovered and abundant materials collected, scholars discussed the biochronological sequence of Pleistocene faunas and proposed different schemes (e. g. Zhou, 1957; Kahlke and Hu, 1961; Pei, 1980; Ji, 1977; Huang, 1979; Han and Xu, 1985). However, due to the lack of systematic geochronological analyses, it was not possible to describe the temporal and spatial evolution of the " *Ailuropoda-Stegodon* " faunal complex in southern China (Wang et al., 2007).

During the past 20 years, researchers continuously carried out investigations and excavations in the Bubing Basin and Chongzuo in the Guangxi province, further advanced in the study of these Quaternary mammals from karstic caves of southern China, and established the evolutionary sequence of faunas for the Early Pleistocene (Wang et al., 2007, 2014, 2017; Rink et al., 2008; Sun et al., 2014). Despite this, our understanding of the evolution of the large-bodied mammalian faunas in a securely dated context, and their geographical distributions, is still insufficient for the Middle and the Late Pleistocene.

The Late Pleistocene deposits in southern China often yield remains of *Homo sapiens* considered to be the earliest evidence of modern humans in East Asia. Therefore, the age of some key-sites for our understanding of the hominin evolution and dispersal, generated intensive debates. Indeed, researchers face challenges in providing secure chronologies for humans-bearing deposits and their associated faunas in complex karstic environments. For example, the fragmentary human remains of Zhirendong (or Zhiren cave) in south China, have been dated to the initial Late Pleistocene, >100 ka, by the Uranium-series (U-series) method and faunal correlation with notably the first appearance of *Elephas maximus* (Jin et al., 2009; Liu et al., 2010; Cai et al., 2017). However, recent dating results suggest that these human fossils and associated mammals were deposited during the Middle Pleistocene, between ~190 and 130 ka (Ge et al., 2020). In 2015, Liu and his colleagues reported the discovery of 47 isolated teeth of modern humans in the Fuyan cave, associated with *Stegodon-Ailuropoda* components, dated to 80-120 ka based on U-series results of flowstones. They also claimed that it represented the earliest fossil evidence of modern human in East Asia (Liu et al., 2015). Recently, Sun et al. (2021b) questioned the age of the Fuyan site. They argued that, even if new U-series measurements of flowstones suggest a range of 168 to 70 ka, the age of some human teeth based on ancient DNA analysis and direct AMS 14C dating, is rather Holocene. They further emphasized, by applying the optically stimulated luminescence

dating method (OSL) on sediments and that of AMS 14C on both mammal teeth and charcoal, that the Fuyan site is much younger than previously proposed (but see Martinón-Torres et al., 2021). In addition to the need for using multiple dating techniques on both fossils and deposits, both examples also show that, given the state of knowledge, one cannot rely on the composition of faunal assemblages as biochronological landmarks, due to the confusion between the Middle and the Late Pleistocene records. Undoubtedly, the lack of age precision limits our understanding of the environmental changes which accompanied the history of hominins (*Homo erectus*, *Homo sapiens*, Denisovans) in the region. Thus, until a reliable biochronological sequence is established with more comprehensive faunal records, it is difficult to recognize Late Pleistocene from Middle Pleistocene mammalian faunas in cave deposits of southern China.

In an attempt to highlight the successive events that affected the *Ailuropoda-Stegodon* faunal association, it is also important, given its wide distribution in the Indochinese subregion, from southern China to the Indochinese Peninsula, to consider the biogeographical context. Few studies focused on megafauna and hominin extinction in overall Southeast Asia over the Pleistocene (Louys et al., 2007; Louys and Roberts, 2020), likewise for studies on species dynamics (migration, replacement by new species or populations, etc.) between southeast Asian mainland and southern China, in a fluctuating climate (e. g. Suraprasit et al., 2020; Bacon et al., 2021). Overall, what we know, at a continental scale, is that *Gigantopithecus*, *Pachycrocuta*, *Stegodon, Palaeoloxodon, Hexaprotodon,* and *Megatapirus* went extinct at various periods in the Pleistocene (Louys et al., 2007), that *Crocuta ultima, Ailuropoda baconi,* and *Stegodon orientalis* went extinct just before the onset of the Holocene (Turvey et al., 2013; Bacon et al., 2018a), whereas the distribution ranges of some modern taxa changed dramatically, like those of *Tapirus indicus, Pongo Pygmaeus* and *Sus barbatus* which moved southward (Corbet and Hill, 1992). All these changes led to the modern distribution pattern of megafaunas. To date, the earliest modern fauna in the mainland of Southeast Asia has been dated to 70-60 ka in northern Vietnam (Duoi U'Oi cave, Bacon et al., 2008). However, the use of this fauna in the overall history of East Asia, along with those at the transition between the Middle and the Late Pleistocene, Nam Lot in Laos (86–72 ka, Bacon et al., 2015) and Coc Muoi in Vietnam (147–118 ka, Bacon et al., 2018b), are rarely covered in the reports of southern China (e. g. Liang et al., 2020a; Zhang et al., 2014; Jin et al., 2009).

Located at the intersection between East and Southeast Asia, the Guangxi Zhuang Autonomous Region has produced the richest Quaternary mammalian fossil assemblages in cave deposits from the Early Pleistocene to the Late Holocene, which studies shed light on the quaternary mammalian evolution in relation to large environmental changes. Interestingly, most fossil sites have been found so far in the karst landscape and nearby river valleys, as well as in basin margins in northwestern Guangxi, while few reports mention the discovery of quaternary mammalian fossils in southeastern Guangxi. Indeed, this area is covered by plains and hilly landscapes, limiting the palaeontological and environmental researches in the region (Fig. 1).

Here, we report the discovery of a new cave site in southeastern Guangxi, the Mocun cave. In 2000, numerous mammalian fossils, including a complete skeleton of *Elephas maximus*, were extracted in a karstic cave near the Mocun village, Qinzhou, Guangxi, when local villagers were mining for stones. With the collaboration of the Guangxi Natural History Museum and the Pubei County Museum, the sedimentary deposits were completely excavated and the stratigraphy recorded. Based on the absolute dating performed on calcitic concretions and dentin of fossil teeth, we dated the fossiliferous layers. We analysed the assemblages composed of teeth of small- to

large-sized mammals collected in the richest layers of the sequence, using a classical zooarchaeological approach. We conducted a taphonomic study in order to identify the abiotic and biotic agents that may have contributed to the composition and preservation of the assemblage. We also used age categories of some taxa in order to emphasize potential prey preferences of large predators. Finally, we discussed the contribution of the mammalian fauna of Mocun to the Late Pleistocene biogeographical history of the region.

2. Geology and chronology

2.1. Location and geological context

The Mocun cave (109°53'11"E, 22°60'15"N) is located in a karst peak about 500 m southwest of the Mocun Village, Pubei, Qinzhou, southeast of the Guangxi Zhuang Autonomous Region (Fig. 1). The surrounding landscape is dominated by low-lying granite hills, developed in the late Indosinian, with scattered karst limestone peaks (Guangxi Bureau of Geology and Mineral Resources，1985). These tower karsts near Mocun are formed of a grey to white thick dolomitic limestone unit dated to the Middle and Upper Carboniferous. The alluvial plain around the limestone peak deposits weathered latosol or brown calcareous soil, now used as farmland (Long, 1994). The Mocun cave is in a small basin among hills, a nearby small tributary flows 20 km north into the Yujiang River.

The tower karsts near Mocun showing the last stage of karst process, have been affected by strong carbonate dissolution that shaped caves of different structures and sizes. Inside the karstic system, speleothems are composed of encapsulating stalactites and stalagmites. The sediments were transported by rainwaters and deposited in the lower part of the karstic network, forced by intense dissolution and slope deposition. Rain fell across the surface of the Mountain, and passed through the karstic cave system, allowing the final deposition of sediments on the surrounding plain. The breccia deposits are mostly composed of weathered sandy clays and clasts transported by waters inside the cave. Indeed, fluvial alluviums (pebbles and sand) are absent. The limestone blocks may have fallen from the cave ceiling.

The Mocun cave site is located on the side of an isolated limestone peak. Due to the long exploitation of the cave for cement, the original landform of the site is unclear. However, some quaternary sediments are fortunately preserved in the east and west parts of the mining pit (Fig. 2). In the east, the upper part of the sediment and the ceiling (if there is), were removed for digging down. In the remaining deposit, abundant large fossil bones were collected from a breccia layer, and subsequently identified as belonging to one individual of *Elephas maximus*. Nevertheless, small pieces of fossil bones and teeth are rare in this locus. Based on the special nature of sediments, we speculate that this is more likely a fissure deposit. In the west, the sediment was well-preserved, showing an undisturbed sequence of deposition with several small and fragmentary bones and abundant mammalian teeth of various taxa. The bones are however difficult to identify taxonomically. This study focuses on materials, mostly isolated teeth, recovered in the western part of the cave.

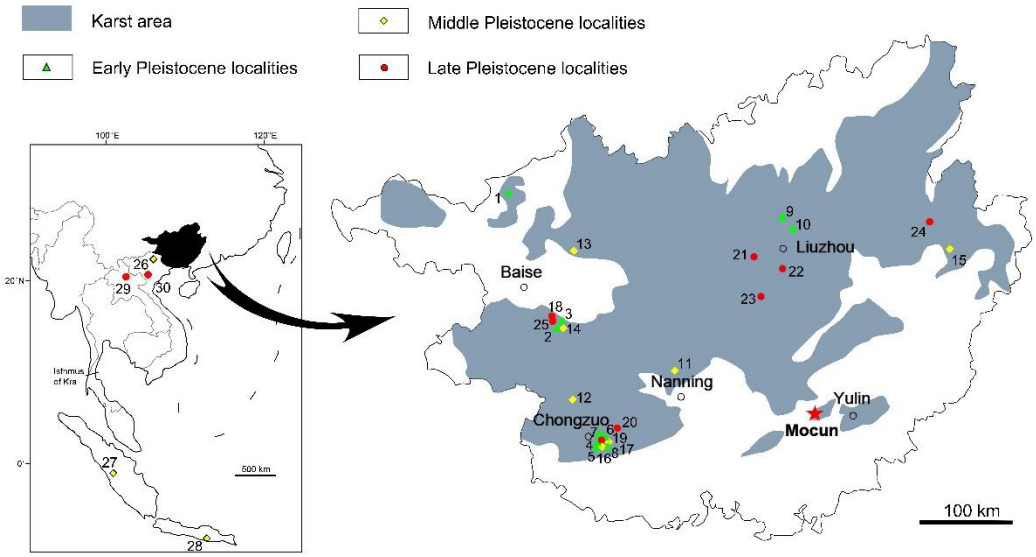

Fig. 1. Distribution of the karst area in Guangxi and location of pleistocene mammalian fossil localities; The other mammalian sites used in this article have been noted on the map of southeast Asia.

Early Pleistocene: 1, Jinyin cave (Jin et al., 2007); 2, Chuifeng cave (Wang, 2009); 3, Mohui cave (Wang, 2005); 4, Sanhe cave (Jin et al., 2008); 5, Queque cave (Jin et al., 2014); 6, Juyuan cave (Dong et al., 2010); 7, Baikong cave (Jin et al., 2014); 8, Yanliang cave (Zhang et al., 2016); 9, Liucheng (Pei,1957); 10, Bijiashan cave (Han et al., 1975); Middle Pleistocene: 11, Wuming (Zhang et al., 1973); 12,Daxin cave (Pei and Woo, 1956); 13, Bama (Zhang et al., 1975); 14, Wuyun cave (Chen et al., 2002); 15, Diaozhongyan cave (Liang et al., 2020a); 16, Hejiang cave (Zhang et al., 2014); 17, Yixiantian cave (Pan, 2021); Late Pleistocene: 18, Dingmo cave (Li et al., 1985); 19, Zhiren cave (Jin et al., 2009); 20, Nanshan cave (Wang and Mo, 2004); 21, Ganxian cave (Liang, 2020b); 22, Liujiang (Woo, 1959); 23, Qilinshan cave (Jia and Woo, 1959); 24, Jimuyan cave (Wang et al., 2011); 25, Luna cave (Bae et al., 2014). Southeast Asia: 26, Coc Muoi (Bacon et al., 2018b); 27, Ngalau Gupin (Smith et al., 2021); 28, Punung (Storm et al., 2005; Westaway et al., 2007); 29, Nam Lot (Bacon et al., 2015); 30, Duoi U'Oi (Bacon et al., 2008).

Fig. 2. Photos of the Mocun site: (a) Landscape of the surrounding area and location of the Mocun cave; (b) Excavation and karstic deposit in the Mocun cave.

2.2. Stratigraphy

Eight stratigraphic layers have been identified, from the top to the base of the sequence (Fig. 3):

L1 Light brown thick sandy clay. 130 cm;

L2 Light brown sandy clay with limestone interbedded with breccias of ~10 cm. 40 cm;

L3 Grey layered flowstone. 10–30cm;

L4 Brown silty clay which yielded bone fragments and small-sized fossil rodents. 70 cm;

L5 Yellow silty clay without fossils. 20 cm;

L6 Black iron-manganese encrustations showing a sintered lower surface. 20 cm;

L7 light brown loose sandy clay which yielded plentiful of small- to large-sized mammalian fossil teeth. 100 cm;

L8 brown sandy clay which contained an upper fossil-rich part (~60 cm) and a lower fossil-sterile part (~90 cm). Total thickness of 150 cm.

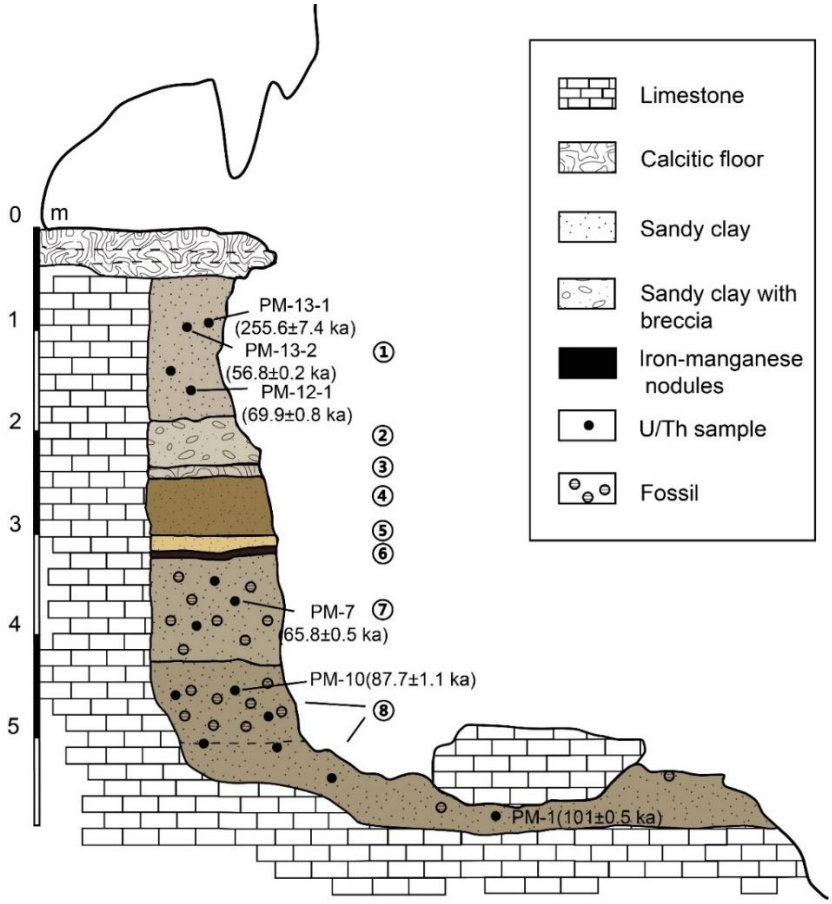

Fig. 3. Sedimentary filling of the west wall in Mocun cave (L8 is divided into rich and poor zones, at 2.8 meter below L3).

3. Methods and material

3.1. Excavation

In 2000, our excavation concentrated on the west part of the cave, in an area of about 5 m^2, and excavated by intervals of 10 cm. Hammer, chisel, bamboo-stick, brush were used to excavate. Moreover, 50 kg of sediments were water-screened to collect micromammals using 35 mm mesh sieves. In the present article, however, our analysis only focuses on large mammals, that of micromammals will be the subject of a separate article.

3.2. U-series dating

To constrain the chronological range of the stratigraphic sequence, several samples extracted from the different deposits were selected: soda straw stalactites and teeth. They have been dated by the classic $^{238}U/^{234}U/^{230}Th$ disequilibria method (Edwards et al., 2003; Chabaux et al., 2003). The soda straw stalactites were respectively obtained from L1 (PM-12), L7 (PM-11) and L8 (PM-10). The straw stalactites, which formed at the ceiling and fell in the sediments after their fracture, thus represent the maximum age of these deposits. Considering the stratigraphy, several mammal dentine samples were also selected from L1 (PM-13-2), L7 (PM-7), L8 (PM-6), at the different

depths of 2.4 m and 2.9 m below the Layer 3, and in the Layer 8 (PM-4、PM-2-1、PM-2-2、PM-2-3、PM-1) (Figs. 3 and 4). The U-series dating of teeth provide the minimum age of the fauna within the three layers, L1, L7 and L8 (Table 1).

The carbonate samples without recrystallization or secondary carbonate precipitate were cleaned by dental drill and ultraphonic cleaner to remove attached detritus. 100 mg cleanest carbonate or 1.5 mg pure dentine samples were handpicked to mix with ^{229}Th–^{233}U–^{236}U triple spike with known quantity after dissolution in 14 N HCO_3. After complete mixture, they were heated at 120 ◦C to dry up, and re-dissolved for Th and U separating. The details of chemical pre-treatment procedures have been described in Shao et al. (2017, 2019). Analytical procedures were carried out by a Neptune multiple-collector ICPMS at the School of Geography Science, Nanjing Normal University. Finally, the U-series ages were estimated by Monte-Carlo simulations (Shao et al., 2019) and adjusted with the bulk crustal 232Th/238U concentration ratio of 3.8 to exclude possible contamination.

3.3. Identification of faunal remains

Due to the particular preservation of the Mocun assemblage, which consists of a majority of isolated teeth, rare remains of maxillae and mandibles and a few bones, the identification of species is based on isolated teeth. Remains of long bones, mostly fragmentary diaphysis gnawed by rodents, although important to understand the taphonomy at the site, have no taxonomic interest.

Taxa have been identified at the species level, when possible, using morphology and dimensions of specimens, and the number of identified specimens (NISP) by taxon has been estimated. The Fisher's exact test was performed on NISP using the R version 4.0.5.

By convention, we used minuscule letters for lower teeth (i/c/p/m) and majuscules for upper teeth (I/C/P/M).

The composition of the Mocun fauna has been compared with that of southeast Asian faunas of known age, from the Middle to the Late Pleistocene: Middle Pleistocene sites of Hejiang cave, Ganxian cave, Diaozhongyan cave in southern China (Zhang et al., 2014; Liang, 2020b; Liang et al., 2020a); Coc Muoi in northeastern Vietnam (Bacon et al., 2018b), Ngalau Gupin in Sumatra (Smith et al., 2021); Punung in Java (Storm et al., 2005; Westaway et al., 2007); Late Pleistocene sites of Zhiren cave (Jin et al., 2009) and Fuyan cave (Li et al., 2013) in southern China, Nam Lot in northeastern Laos (Bacon et al., 2015) and Duoi U'Oi in northern Vietnam (Bacon et al., 2008) (Fig. 1, Table 2).

3.4. Taphonomy

Our taphonomic analysis focuses on the selective preservation of teeth in the most abundant taxa (Cercopithecidae, Ursidae, Suidae, Cervidae) using the frequencies of upper *vs* lower teeth and deciduous *vs* permanent teeth, and on the nature and intensity of damages on teeth.

We analysed the damage on teeth in order to assess the factors, either biotic (rodents and carnivores) or abiotic (water flows), that may have contributed to the preservation of the assemblage. In Asia, among rodents, porcupines proved to be important collectors of skeletal elements, including crania and mandibles, of a large array of mammals (Bacon et al., 2015). They used to drag to their dens remains of carcasses left at the site (Brain, 1981). Their signature consists of grooves and characteristic chisel marks on bones and roots of teeth and exposed dentine, and

which size is consistent with that of their incisors. The damages left by porcupines cannot be confused with damages caused by carnivores, particularly hyenas, which often consist of breakage on teeth. Rodents gnaw bones and dentine of animals to extract nutrients or to wear continuously their incisors (Brain, 1981). We used NISP to calculate the gnawing frequency of teeth by taxon (Cercopithecidae, Ursidae, Suidae, Cervidae), and examined the role these collectors may have played in the Mocun cave. Some other types of damage on the surface of teeth have also been assessed to analyse the intensity of water flows during processes of transport and deposition in the cave.

We also attempted to estimate age classes of individuals, juvenile and adult, using two types of minimum number of individuals (MNI). The first one represents the frequency of the most common type of tooth within deciduous and permanent teeth, either left or right, upper or lower. This index is cited as MNIf (frequency). MNIc (combination) is used by combining the type of tooth and the wear stage, and allows the distinction between young adult and adult in Artiodactyla and Perissodactyla.

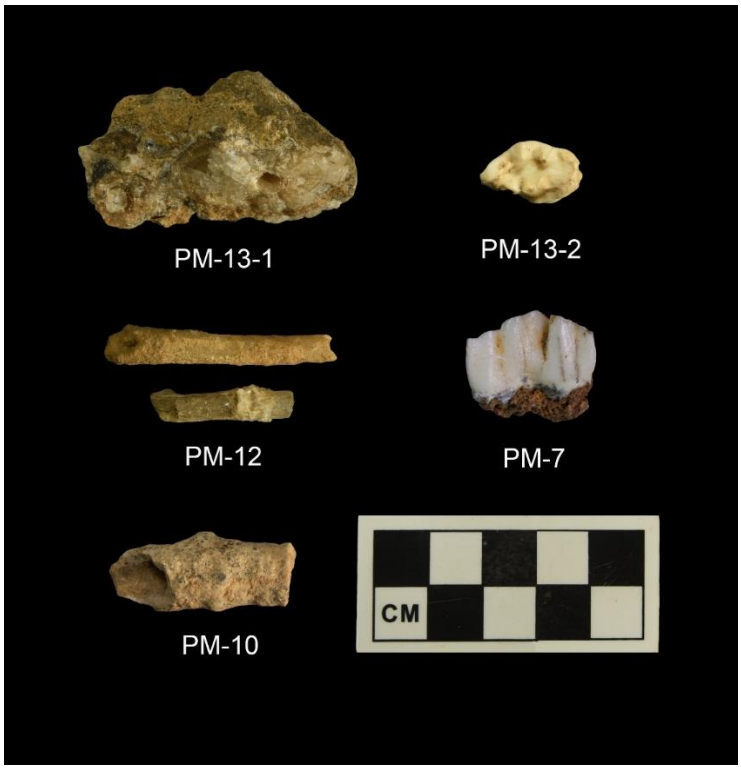

Fig. 4. Samples used for U-Series dating.

4. Results

4.1. Dating results

The maximum age of L1 ranges between 57 ka and 69 ka, restricted by the dating of dentine samples and straw stalactites samples, respectively. However, because of the complex life progress of the straw stalactites from L7, it is unable to limit the maximum age. Combining the dating results of each sample, the minimum U-series age for L7 is 65.8±0.5 ka, while the maximum age for L8 is

87.7±1.1 ka. Thus, based on U-series results of L7 and L8, the dominant fossil-bearing layers range between 66 ka and 86 ka. The bottom of L8 fossil-sterile part provides an earlier age of ~101 ka, which is consistent with the dating of the subjacent layers (Table 1). To determine the age of fossils, 12 dentine samples were selected. For all, the dentine provided minimum ages younger than those of straw stalactites. Therefore, it is reasonable to infer that the mammal fauna is contemporaneous with the deposits.

4.2. The composition of the fauna

A total number of 543 isolated teeth of large mammals (NISP), all unearthed in the western part of the Mocun cave, have been identified, either at the genus or species level.

4.2.1. Primates

Macaca sp. A set of 97 isolated teeth was collected, including upper and lower teeth and covering all permanent tooth types except maxillary canine and p3. Eighty teeth are from L8, 8 teeth are from L7, and the other 9 specimens are from the ground level.

The upper molars, low-crowned and bilophodont, show the typical morphological pattern of *Macaca*. Four pointed cusps are connected by transverse ridges and the protocone is well-developed. The anterior loph is larger than the posterior one, while the mesial fossa is of similar size as the distal fossa. The lower molars (m1/m2) are rectangular in outline, with a wide and deep fossa between transverse ridges. A buccal cingulum is present on some teeth. These morphological characteristics are close to those of extant macaques.

In relation to dimensions of teeth (Table 3-1), there is a large overlap between macaque species (Fooden, 1990; Swindler, 2002). However, the macaque from Mocun is larger than that of Coc Muoi (Bacon et al., 2018b) and Duoi U'Oi (Bacon et al., 2008), and appears closer to the species *Macaca arctoides* from Chinese sites and, to a lesser extent, to *M. mulatta* and *M. nemestrina* with a small overlap of m3 (Takai et al., 2014). Therefore, we preferentially assign the Mocun specimens to *Macaca* sp. (Fig. 5).

Trachypithecus sp. Two lower m3s of colobine monkeys were unearthed in Mocun cave from L7 and L8. Both molars have higher and more pointed cusps than those of macaques. One molar is smaller in size that those of *Macaca* sp. (Table 3-1). The four main cusps are connected by transverse lophs with a hypoconulid positioned buccally. The median lingual notch is deep (Fig. 5).

Hylobates sp. Two isolated permanent teeth (one M1/M2 and one canine) attributed to the genus *Hylobates* were collected from L8. The morphology of the Mocun specimens is similar to that of extant gibbons (Frisch, 1965). The upper molar (M1 or M2) displays four main cusps. The buccal cusps are mesial to lingual cusps. A crista obliqua connects the protocone and the metacone. There is no distinct cingulum. Based on a small sample, we cautiously retain an attribution to *Hylobates* sp. (Fig. 5).

Pongo sp. An upper molar attributed to *Pongo* was discovered in L8. This specimen has two mesial and distal wear facets, as for M1 and M2. Metacone and hypocone are reduced in comparison to mesial cusps, and the crown has a rhombic shape. So, we identified the tooth as a left M2. The crown is slightly worn and crenulations are still visible on the occlusal surface. This M2 displays four main cusps, and the metacone is as high as the paracone. Protocone and metacone are joined by the oblique ridge (postprotocrista) and the hypocone is separated by a groove from the other cusps. The mesial and distal fossae are shallow, while the median fossa is wide and deep.

The buccal groove separates the two buccal cusps.

The morphology of the Mocun specimen is similar to that of extant and subfossil orangutans from Indonesia. However, it is larger than living species and its dimensions (Table 3-1) fall within the range of *Pongo pygmaeus weidenreichi* (Zhao et al., 2009；Liang et al., 2020b). Based on a single collected tooth, it is temporarily identified as *Pongo* sp. (Fig. 5).

4.2.2. Rodentia

Large rodents are represented by Hystricids. The set of teeth of the porcupines from Mocun cave can be divided into two species.

Hystrix magna: Thirty-two upper and lower isolated permanent teeth of *Hystrix magna* have been identified based on large size and crown height (Table 3-2), while the morphology of the occlusal surface is similar between species (Van Weers and Zheng, 1998). *H. magna* is represented by the specimens from *Gigantopithecus* cave in Liucheng (Pei，1987), a large-sized species in the family of Hystricidae, which ranges between *H. zhengi* (Zheng，1993) and *H. kiangsenensis* (Zheng, 2004). The length and width ranges of some large cheek teeth from Mocun overlap those of Chongzuo and Jianshi (Zheng, 2004; Guo, 1997). Thus, we assign these specimens to *H. magna* (Fig. 6).

Hystrix cf. *subcristata*: Fifty-nine permanent teeth, incisors, premolars and molars, are attributed to *Hystrix* cf. *subcristata*. They were collected from the ground, and from L7 and L8. These specimens are smaller than those attributed to *H. magna*, and larger than those of *H. lagrelli.* The size ranges of both the Early to mid-Late Pleistocene *H. kiangsenensis* and the extant *H. subcristata* overlap that of the Mocun specimens. However, the Mocun specimens appear more robust, with a larger width than those from Jianshi (Zheng, 2004), and are closer to those of Tianyuan cave (Tong, 2005) and Duoi U'Oi (Bacon et al., 2008). Overall, we retain for the Mocun teeth an attribution to *H.* cf. *subcristata* (Fig. 6).

Table 1. U-series ages of Mocun cave.

Number	Sample	Stratum	238U[ppm]	232Th[ppb]	(230Th/238U)	Age[ka]	D234U_0[permil]	Corr.Age[ka BP]
PM-13-1	stalactites	L1	0.0358±0.00007	4.2486±0.0192	0.9712±0.0044	258.7856±7.2016	113.7213±9.6026	255.6299±7.3548
PM-13-2	dentine	L1	11.6789±0.004	14.1250±1.166	0.5126±0.0015	56.8285±0.2356	284.2648±1.7303	56.8010±0.2359
PM-12-1	soda straw stalactites	L1	0.0318±0.00005	1.9792±0.0097	0.6657±0.0025	71.1517±0.4735	431.2994±4.8156	69.8779±0.7933
PM-12-2	soda straw stalactites	L1	0.0775±0.0001	0.7949±0.011	1.3493±0.0035	163.3232±1.1454	973.3911±6.0683	163.1716±1.1475
PM-7	dentine	L7	4.3928±0.005	47.5479±0.3597	0.5868±0.0030	66.0761±0.5091	320.9125±3.5614	65.8371±0.5218
PM-11	soda straw stalactites	L7	0.4583±0.0001	4.6604±0.0255	0.7836±0.0011	136.1029±0.4505	123.7036±1.1132	135.8389±0.4690
PM-14	dentine	L7	2.4139±0.0034	41.8217±0.3795	0.2496±0.0015	27.0702±0.2141	138.0450±3.7664	26.6256±0.3067
PM-6	dentine	L8	6.7616±0.002	1.9151±0.4135	0.4708±0.0009	43.4535±0.1062	459.4447±1.3257	43.4478±0.1063
PM-10	soda straw stalactites	L8	0.0456±0.00009	2.5846±0.0232	0.6869±0.0036	89.0499±0.9202	263.8562±6.3452	87.7369±1.1260
PM-5	dentine	L8-4.3m	4.9549±0.002	1.0594±0.4718	0.5364±0.0013	61.5110±0.2291	267.0795±1.8763	61.5058±0.2291
PM-3-1	dentine	L8-4.8m	2.3881±0.002	1.6791±0.4718	0.2656±0.0010	28.1572±0.1441	171.4394±2.7255	28.1393±0.1444
PM-3-2	dentine	L8-4.8m	4.2333±0.0047	10.4083±0.3711	0.5430±0.0018	60.7090±0.3323	296.8594±3.5328	60.6537±0.3332
PM-4	dentine	L8-4.8m	6.6913±0.002	0.8860±0.6136	0.5504±0.0014	63.1593±0.2530	276.0967±2.2736	63.1557±0.3251
PM-2-1	dentine	L8-5m	10.4164±0.003	‘-0.1264±0.6897	0.5659±0.0010	67.5189±0.1963	249.5762±1.5493	67.5190±0.2455
PM-2-2	dentine	L8-5m	13.4715±0.0057	16.6864±1.2089	0.5308±0.0014	60.7121±0.2794	265.6248±3.0373	60.6835±0.2797
PM-2-3	dentine	L8-5m	5.8082±0.0067	19.3895±0.5173	0.5964±0.002	69.7989±0.3962	290.0352±3.5015	69.7234±0.3978
PM-1	dentine	L8-5.3m	6.7266±0.003	8.3635±0.8081	0.7756±0.0018	101.0662±0.4587	332.6666±2.5551	101.0390±0.4588

Table 2-1. Composition of the Mocun faunal assemblage (Artiodactyla, Perissodactyla, and Proboscidea) compared with that of some late Middle Pleistocene to Late Pleistocene sites in Southern China: Hejiang cave (Zhang et al., 2014), Ganxian cave (Liang, 2020b), Diaozhongyan (DZY) cave (Liang et al., 2020a), Zhiren cave (Jin et al., 2009), and Fuyan cave (Li et al., 2013). Names in bold indicate global extinction; The asterisk (*) indicates local extinction.

	Hejiang cave 320-400 ka	**Ganxian cave 160-360 ka**	**DZY cave 205-231ka**	**Zhiren cave 116-106 ka (?) 190-130 ka (?)**	**Fuyan cave 80-120ka**	**Mocun cave 66-101 ka**
Megalovis guangxiensis	√	√		√		
Rusa (Cervus) unicolor/sp.	√	√	√	√	√	√
Muntiacus reevesi						√
Muntiacus muntjak/sp.		√	√		√	√
Bubalus bubalis				√		
Bos (Bibos) sp.	√	√			√	√
**Capricornis sumatraensis*		√			√	
Caprinae gen. et sp. indet.			√		√	√
Sus xiaozhu	√	√		√		√
Sus scrofa	√	√	√	√	√	√
Megatapirus augustus				√	√	√
Tapirus sinensis	√	√	√			√
Rhinoceros sinensis	√	√	√	√		
**Rhinoceros sp.*						√
**Dicerorhinus sumatrensis*					√	
Stegodon orientalis/sp.	√	√	√		√	√
Elephas kiangnanensis				√		
**Elephas maximus*		√		√	√	√

Table 2-2. Composition of the Mocun faunal assemblage (Carnivora, Primates, and Rodentia) compared with that of some late Middle Pleistocene to Late Pleistocene sites in Southern China: Hejiang cave (Zhang et al., 2014), Ganxian cave (Liang, 2020b), Diaozhongyan (DZY) cave (Liang et al., 2020a), Zhiren cave (Jin et al., 2009), and Fuyan cave (Li et al., 2013). Names in bold indicate global extinction; The asterisk (*) indicates local extinction.

	Hejiang cave 320-400 ka	**Ganxian cave 160-360 ka**	**DZY cave 205-231ka**	**Zhiren cave 116-106 ka (?) 190-130 ka (?)**	**Fuyan cave 80-120 ka**	**Mocun cave 66-101 ka**
**Cuon antiquus*					√	
Cuon sp.						√
Arctonyx collaris (rostratus)		√	√	√	√	√
Paguma sp.				√		
Viverra sp.				√	√	√
**Felis(Panthera) tigris*	√	√			√	
Felis(Panthera) sp.				√		
Paradoxurus cf. *hermaphroditus*						√
Neofelis nebulosa						√
Panthera pardus	√			√	√	
Crocuta ultima					√	√
⁎Crocuta/Hyaena sp.	√					
**Ailuropoda melanoleuca baconi*	√	√	√		√	
**Ailuropoda sp.*						√
Ursus thibetanus	√	√	√	√	√	√
Gigantopithecus blacki	√					
**Pongo pygmaeus*		√		√		
**Pongo* sp.						√

Nomascus/Hylobates sp.	√		√	√	√	√
Macaca sp.	√	√	√	√	√	√
Trachypithecus sp.	√	√	√	√	√	√
Hystrix magna						√
Hystrix kiangsenensis		√				
Hystrix subcristata		√	√		√	√
Homo sapiens				√		

Table 2-3. Composition of the Mocun faunal assemblage (Artiodactyla, Perissodactyla, and Proboscidea) compared with that of some late Middle Pleistocene to Late Pleistocene sites in Southeast Asia: Coc Muoi (Bacon et al., 2018b), Nam Lot and Duoi U'Oi (Bacon et al., 2015), Ngalau Gupin (Smith et al., 2021), and Punung (Storm et al., 2005; Storm and de Vos, 2006). Names in bold indicate global extinction; The asterisk (*) indicates local extinction.

	Coc Muoi 117-148 ka	**Nam Lot 72-86 ka**	**Duoi U'Oi 60-70 ka**	**Mocun cave 66-101 ka**	**Ngalau Gupin 115-160 ka**	**Punung 118-128 ka**
Tragulus sp.					√	
Rusa (Cervus) unicolor/Rusa sp.	√	√	√	√	√	√
Muntiacus reevesi				√		
Muntiacus muntjak/Muntiacus sp.	√	√	√	√	√	√
Bos (Bibos) sp.		√	√	√	?	
Bos sauveli	√					
Bubalus bubalis/B. arnee		√				√
**Capricornis sumatraensis/Capricornis* sp.	√	√	√		√	√
Caprinae gen. et sp. indet.				√		
Sus xiaozhu.				√		
Sus scrofa	√	√	√	√	√	√
**Sus barbatus*			√		√	
Megatapirus augustus.	√			√		
Tapirus sinensis.				√		
**Tapirus indicus/Tapirus* sp.	√	√	√		√	√
**Rhinoceros* sp.		√	√	√		
**Rhinoceros unicornis*	√	√	√		√	
**Rhinoceros sondaicus*	√	√	√		√	√

**Dicerorhinus sumatrensis*	√		√		√	√
***Hexaprotodon* sp.**					√	
***Stegodon orientalis/Stegodon* sp.**	√	√		√		
**Elephas maximus/Elephas* sp.	√	√	√	√	√	√

Table 2-4, Composition of the Mocun faunal assemblage (Carnivora, Primates, and Rodentia) compared with that of some late Middle Pleistocene to Late Pleistocene sites in Southeast Asia: Coc Muoi (Bacon et al., 2018b), Nam Lot and Duoi U'Oi (Bacon et al., 2015), Ngalau Gupin (Smith et al., 2021), and Punung (Storm et al. 2005; Storm and de Vos 2006). Names in bold indicate global extinction; The asterisk (*) indicates local extinction.

	Coc Muoi 117-148 ka	**Nam Lot 72-86 ka**	**Duoi U'Oi 60-70 ka**	**Mocun cave 66-101 ka**	**Ngalau Gupin 115-160 ka**	**Punung 118-128 ka**
Cuon sp.				√		
**Cuon alpinus/C.alpinus antiquus*	√	√	√			
Arctonyx collaris/A. collaris rostratus			√	√		
Viverra zibetha/Viverra sp.		√	√	√		
Viverra megaspila			√			
Paradoxurus sp.					√	
Paradoxurus cf. *hermaphroditus*				√		
Neofelis nebulosa		√	√	√		√
Panthera pardus			√			
Felis (Panthera) sp.						
**Felis (Panthera) tigris*	√		√		√	√

Crocuta ultima		√		√		
**Helarctos malayanus*	√		√		√	√
Ursus sp.						
Ursus thibetanus//U. thibetanus kokeni	√	√	√	√		
**Ailuropoda melanoleuca baconi/fovealis*	√	√				
**Ailuropoda sp.*				√		
**Pongo pygmaeus*		√	√			√
**Pongo devosi*	√					
**Pongo* sp.				√	√	
Symphalangus syndactylus						√
Hylobates sp.	√		√	√	√	√
Macaca sp.	√		√	√	√	√
Trachypithecus sp.				√		√
Nasalis sp.					√	
Hystrix subcristata				√		
Hystrix brachyura/Hystrix sp.		√	√		√	√
Atherurus macrourus					√	
Hystrix magna				√		
Homo sapiens						√
Homo sp.			√			

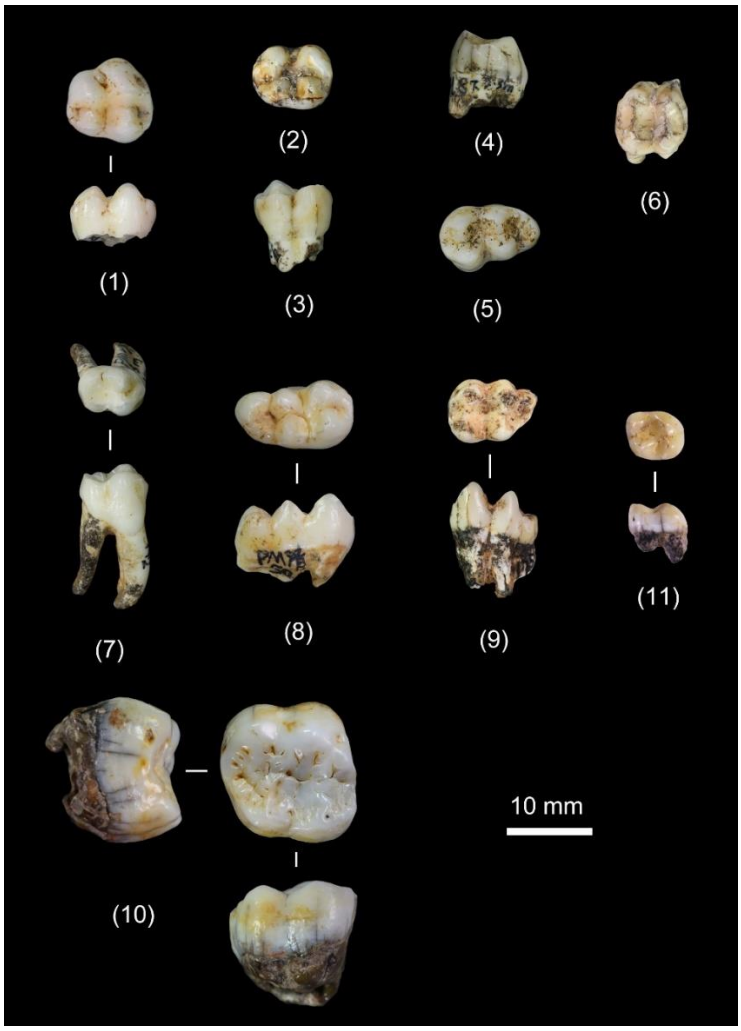

Fig. 5. Primates from Mocun cave. *Macaca* sp.: (1) left M3 (PMWUL8-099) in occlusal and lingual view; (2) left M2 (PMWLL8-130) in occlusal view; (3) left M2 (PMWLL8-164) in buccal view; (4) left m2 (PMWLL8-168) in mesial view; (5) left m3 (PMWLL8-145) in occlusal view; (6) right M1 (PMWD-51) in occlusal view; (7) right p4 in occlusal and buccal view (PMWLL8-142); (8) left m3 in occlusal and lingual view (PMWD-50). *Trachypithecus* sp.: (9) right m3 in occlusal and lingual view (PMWLL8-175). *Pongo* sp.: (10) left M2 in occlusal, distal and buccal view (PMLL8-224). *Hylobates* sp.: (11) right M1 (PMWLL8-174) in occlusal and distal view.

Table 3-1. Dimensions of measurable Primates teeth from Mocun cave (mm). MD, mesiodistal; BL, Buccolingual.

Teeth	N	Length (MD) Range	x	Width (BL) Range	x
Macaca sp.					
P3	13	4.97-6.32	5.81	6.1-8.29	7.04
P4	6	5.88-7.52	6.56	6.85-8.46	7.65
M1	20	6.69-10.07	8.22	6.68-9.45	7.98
M2	15	9.23-10.45	9.65	7.77-9.83	8.91
M3	6	8.35-10	9.55	6.52-10.29	9.05
p4	4	7.37-7.55	7.49	5.71-6.57	5.99
m1	8	7.79-10.36	8.32	6.03-8.69	6.92
m2	4	9.31-9.84	9.6	8.4-8.88	8.65
m3	7	11.68-13.49	12.75	7.31-9.5	8.08
Trachypithecus sp.					
m3	1	/	10.04	/	7.19
Pongo pygmaeus					
M2	1	/	15.08	/	16.01
Hylobates sp.					
M1	1	/	6.34	/	7.53

4.2.3. Proboscidea

Stegodon orientalis: Five permanent and one deciduous teeth with low crowns, as well as isolated lophs, were found in L7 and L8. These isolated lophs are too fragmentary to determine the tooth in the dentition. One maxillary P4 only preserved four ridge-shaped lophs and a half loph. The two middle lophs are sightly curved and worn, and the last one is narrower. The maximum width of the crown is 74.45 mm. The outline of two lower molars are rectangular, and convex in lingual view. The lophs positioned at the medial and distal ends of the teeth are much less developed. The maximum width of incomplete crowns varies from 77.26 to 80.48 mm. The morphology and dimensions of the Mocun specimens are consistent with *Stegodon* described at Yenchingkou and Yangjiawan (Colbert and Hooijer, 1953; Tong et al., 2018), and supposed to be *S. orientalis* (Fig. 6).

Elephas maximus: Two permanent teeth, two milk teeth, and three isolated lamellae, can be clearly assigned to *Elephas*. One deciduous tooth is highly worn with a smooth occlusal surface (Fig. 6 (9)). Eight to nine lamellae are preserved and covered by cement. The crown is high as in *Elephas*. Lamellae are closely aligned (vs *Stegodon*) with a U-shape valley between them. This fragmentary specimen is 73.35 mm long, with a measurable maximum width of 35.08 mm. These characteristics and dimensions are consistent with DP3/dp3 of *Elephas maximus* described by Tasumi (1964) and Roth and Shoshani (1988). The characteristic that points to *E. maximus* rather than to *E. namadicus* is the number of lamellae (n = 9) in the DP3/dp3 of Mocun (Bacon et al., 2018b). On identifiable deciduous teeth, the loxodont sinus is absent and the enamel loops are aligned and nearly parallel.

These morphological characteristics are similar to those observed on the specimens from Liucheng and Zhiren cave (Pei, 1987; Wang et al., 2017).

The two incomplete permanent upper/lower molars are elongated with thin lamellae. The h/w index from one measurable lower molar is 212 indicating a high crown, which is close to the data of *E. maximus* from Coc Muoi (Bacon et al., 2018b). Therefore, we assigned these specimens to *Elephas maximus* (Fig. 6).

4.2.4. Carnivora

Arctonyx collaris cf. *rostratus:* Three teeth of a Mustelid attributed to *Arctonyx collaris,* one fragmentary M1 and two p2s or p3s, were recovered at Mocun. Colbert and Hooijer (1953) distinguished a fossil subspecies, morphologically similar but slightly larger than the extant subspecies *A. collaris collaris* (Table 3). The size of the M1 from Mocun falls within the size range of the fossil subspecies, even if there is some overlap with the modern form. On the M1, the distal edge of the talonid is elongated downward, and the hypocone is not developed (Fig. 6).

Cuon sp. Four isolated Canid teeth, including one incisor, two canines and one complete p2, can be allocated to *Cuon* sp., given the small number of specimens. The p2 is large with a well-developed main cusp, elongated posteriorly. The distal cingulum protrudes on the lingual side. The Mocun teeth conform to the dental pattern of the extant species *Cuon alpinus*, and the p2 falls into the size range of *Cuon javanicus antiquus*, rather to those of modern subspecies (Colbert and Hooijer, 1953) (Table 3-2, Fig. 6).,

Crocuta ultima: Only two p2s of similar dimensions were unearthed from L8 and from the ground level. The p2s display a marked distal accessory cuspid separated from the main cusp. In spite of lacking the most discriminating P4, the characteristics of the p2s differ from those of the robust species (*Pachycrocuta*). Their dimensions fall into the ranges of *C. ultima* from Yenchingkuo and Yangjiapo Cave (Colbert and Hooijer, 1953; Lu, 2010) (Table 3-2, Fig. 6).

Viverra sp.: Four isolated teeth, two upper canines, one P4 and one p3, of a Viverrid attributed to *Viverra* sp. were found in L7 and L8. The teeth have been compared to the extant species in southern China, *Viverra zibetha* and the slightly larger *Viverra megaspila*. The P4 shows a developed parastyle close to the paracone, but posterior to the salient protocone. A cingulum is markedly present. These characteristics conform to the pattern of *V. zibetha* and *V. megaspila*, and the dimensions of the Mocun teeth don't differ from those of the modern *V. zibetha*, and from those of one P4 from Duoi U'Oi assigned to *V.* cf. *zibetha* (Bacon et al., 2008). We cautiously assigned these specimens to *Viverra* sp. (Table 3-2, Fig. 6).

Paradoxurus cf. *hermaphroditus*: Only one m1 of *Paradoxurus hermaphroditus* has been identified. The outline of the crown is rectangular. The tooth displays five cuspids low and nearly globular. Based on morphology and dimensions, the Mocun specimen resembles one m1 from Tam Hang (Bacon et al., 2011) (Table 3-2, Fig. 6).

Neofelis nebulosa: One isolated P4 and one p4 of a small Felid assigned to *Neofelis nebulosa* were found in L7. The upper P4 has three buccal cusps, a small parastyle and a blade formed by the paracone and the metastyle of equal height. Between the paracone and the metastyle, the deep carnassial notch presents a distinctive fovea. *N. nebulosa* is a living species in southern China, while only a small number of fossils have been discovered in Middle to Late Pleistocene sites. Mocun cave specimens conform to the dental pattern of the species and to the range of dimensions of *N. nebulosa* identified in Bailong cave and Yangjiawan cave 2 in southern China (Tong et al., 2019;

Jiangzuo et al., 2018) and Duoi U'Oi in northern Vietnam (Bacon et al., 2008) (Table 3-2, Fig. 6).

Ursus thibetanus: The highest number of teeth (n = 18) among Carnivora from Mocun Cave belongs to an Ursid, *Ursus thibetanus*, with one canine, several premolars (p1/p2/p4, P1/P4) and molars (M1/M2, m1/m2/m3). These teeth were mainly excavated from L7. The P4 has salient paracone and metastyle, forming a wide mesiodistal blade. The crown presents a subtriangular outline, and it is surrounded by a cingulum. The M1s are long mesiodistally as in *U. thibetanus*. The M2s show trapezoidal crowns. The metacone is larger than the paracone, and the parastyle is lacking. The molars display an elongated talon and a marked cingulum. The m1 is narrow and long and the mesial parts of the hypoconid and hypoconulid are separated by a distinct constriction. The outline of m2s is rectangular with, on the occlusal surface, an oblique ridge from the protoconid to the entoconid. The ridge between metaconid and entoconid is sharply developed, with two styles. Within extant and fossil ursids, there is a great morphological variation (Erdbrink, 1953). The fossils recorded in the Pleistocene of southern China are considered to be related to *U. thibetanus* (Pei, 1987; Huang and Fang, 1991). Based on the morphology, the Mocun specimens are consistent with the definition of *U. thibetanus kokeni* by Matthew and Granger (1923) and Colbert and Hooijer (1953), and close to those of the Yangjiawan cave 2 (Jiangzuo et al., 2018). In relation to dimensions (Table 3), the Mocun teeth are similar to those from Yenchingkuo and Yangjiapo cave, and to those of living species (Colbert and Hooijer, 1953; Lu, 2010) (Fig. 6).

Ailuropoda sp.: One upper incisor and a fragment of P4 are recorded at Mocun cave (Fig. 6). The Mocun specimens conform to the morphology of the modern panda. However, the teeth allowing a specific attribution are lacking.

Carnivora indet.: Fourteen isolated teeth, mostly canines, of Carnivora are unidentified.

4.2.5. Perissodactyla

Rhinoceros sp.: Thirty-one isolated teeth of a Rhinocerotid were recovered from L7 and L8, a set composed of one half of permanent teeth and one half of milk teeth, all assigned to *Rhinoceros* sp. The morphological characteristics and dimensions of teeth from both layers (L7 and L8) are similar, and represent most likely the same taxon. The antecrochet is present on upper molars, and the depth of the prefossette is the same as that of the postfossette, like in the genus *Rhinoceros.* The rhinoceros from Mocun is distinguished from *R. unicornis, R. sondaicus* and *R. sinensis* from Yenchingkuo and Jianshi (Colbert and Hooijer, 1953; Zheng, 2004), by the presence of a curved ectoloph, a well-developed parastyle, the absence of a crista on upper molars, and the presence of a medifossette on milk teeth.

The dimensions of the Mocun specimens fall between the ranges of *Stephanorhinus* and *Dicerorhinus* (Tong, 2001; Zin-Maung-Maung-Thein et al., 2008; Chen et al., 2012). The teeth morphologically resemble those of *R. fusuiensis* from Yanliang cave (Yan et al., 2014), but appear much less robust with a distinctively smaller width (Table 3). We prefer to assign cautiously these specimens to *Rhinoceros* sp. (Fig. 7). We should add however that, overall, the size of the teeth of the Mocun rhinoceros diverges from the range of known species in southern China and Southeast Asia (Yan et al., 2014; Bacon et al., 2018b), with particularly a smaller width, and may represent a new species.

Tapirus cf. *sinensis*: In Mocun cave, the extinct tapir *Tapirus sinensis* is documented by one lower premolar from L8. The highly worn p4 shows a subrectangular outline, and the hypolophid is wider

than the thick protolophid. The paralophid is reduced in size into a cingulum and there is no crista in the medifossette. *T. sinensis* presents a size similar to that of the Late Pleistocene species *T. indicus*. However, the Mocun specimen has a weak posterior cingulum, that distinguishes it from the p4 of *T. indicus*. The dental pattern and size of the Mocun tooth conforms to *T. sinensis* from Jianshi (Zheng, 2004) (Fig. 7).

Megatapirus augustus: Eight teeth found in L7, a lower incisor, lower deciduous teeth and permanent premolars and molars, including a mandibular fragment with p4 and m1, are attributed to the large tapir *Megatapirus augustus* (Fig. 7). The i1 displays a chisel-shape with a developed lingual groove. The mesiodistal length is 10.23 mm, and the buccolingual width is 9.23 mm. The main difference between the small-sized tapirs (*T. sanyuanensis*, *T. sinensis* and *T. indicus*) and the large *M. augustus* is the dental size. The dimensions of the large tapir from Mocun cave, despite a slightly smaller width, fall within the range of *M. augustus* from Yenchingkuo and Yangjiapo Cave (Colbert and Hooijer, 1953; Lu, 2010), and Coc Muoi (Bacon et al., 2018b) (Table 3) (Fig. 7).

Table 3-2. Dimensions of measurable Carnivora and Rodents teeth in Mocun cave (mm). MD, mesiodistal; BL, Buccolingual.

Teeth	N	Length (MD) Range	x	Width (BL) Range	x
Arctonyx collaris cf. *rostratus*					
p2/3	2	6.61-7.81	7.21	3.22-4.12	3.67
M1	1	/	17.32	/	12.4
Viverra sp.					
P4	1	/	13.37	/	7.31
p3	1	/	8.75	/	4.06
Paradoxurus hermaphroditus					
m1	1	/	5.84	/	6.91
Neofelis nebulosa					
P4	1	/	18.19	/	8.67
p4	1	/	12.29	/	/
Crocuta ultima					
p2	2	16.33-16.41	16.37	11.91-12.62	12.27
Cuon sp.					
p2	1	/	9.28	/	5.05
Ursus thibetanus					
P4	1	/	13.74	/	10.28
M1	4	17.96-19.74	18.75	13.53-16.24	14.63
M2	3	22.84-26.98	25.47	15.84-15.88	15.86
p4	1	/	11.04	/	6.51
m1	1	/	21.32	/	9.27
m2	3	21.67-22.98	22.25	11.77-13.75	12.58
m3	1	/	14.15	/	13.61
Hystrix magna					
P4	2	9.78-10.2	9.99	8.84-9.06	8.95
M1/2	9	8.38-10.43	8.93	6.19-9.41	7.58
M3	7	8.29-10.26	8.97	6.81-10.95	8.29
p4	2	11.03-11.8	11.42	8.09-8.82	8.46
m1/2	2	9.98-10.32	10.15	7.94-8.35	8.15
m3	6	9.08-9.91	9.51	7.31-9.88	8.22
Hystrix subcristata					
P4	7	7.13-9.61	8.72	6.74-8.23	7.43
M1/2	14	6.51-8.6	7.69	6.74-8.41	7.9
M3	5	6.33-8.41	7.35	6.38-8.35	7.1
p4	15	8.11-9.88	9.1	5.86-8.6	7.19
m1/2	9	6.22-9.13	8.18	7.23-9.29	8.2
m3	6	6.91-8.34	7.7	5.84-7.73	6.85

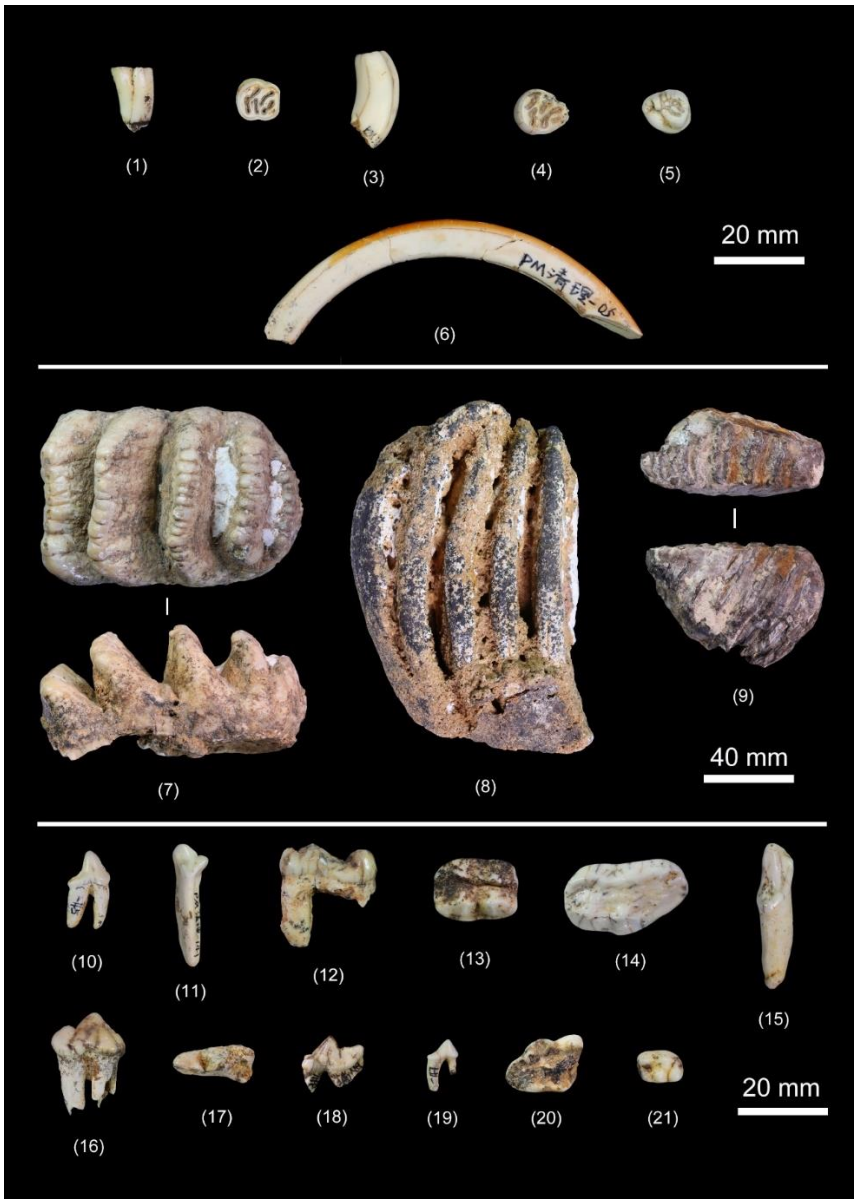

Fig. 6. Rodentia, Proboscidea, and Carnivora from Mocun cave. *Hystrix* cf. *subcristata*: (1) left m2 (PMWD-07) in buccal view; (2) left m1/m2 (PMWLL8-216) in occlusal view; (3) left P4 (PMWD-155) in mesial view. *Hystrix magna*: (4) right m3 (PMWUL8-193) in occlusal view; (5) right M3 (PMWD-157) in occlusal view; (6) left I1 (PMWD-05) in mesial view; *Stegodon orientalis*: (7) left P4 in occlusal and buccal view (PMWD-59); *Elephas maximus*: (8) left lower molar (PMWLL8-028) in lingual or buccal view; (9) deciduous premolar in occlusal and lingual view (PMWD-41). *Cuon* sp.: (10) right p2(PMWD-45) in buccal view; (11) right i3 (PMWD-141) in lingual view. *Ursus thibetanus*: (12) left m1 (PMWUL8-089) in buccal view; (13) left M1 (PMWUL8-085) in occlusal view; (14) right M2 (PMWD-138) in occlusal view. *Ailuropoda* sp.: (15) right I3 (PMWD-143) in lingual view. *Crocuta ultima*: (16) right p2 (PMWLL8-055) in buccal view. *Neofelis nebulosa*: (17) right P4 (PMWUL8-147) in occlusal view. *Viverra* sp.: (18) right P4 (PMWUL8-146) in lingual view. *Arctonyx collaris* cf. *rostratus*: (19) left p2/p3 (PMWD-47) in lingual view; (20) left M1 (PMWLL8-057) in occlusal view. *Paradoxurus* cf. *hermaphroditus*: (21) left m1 (PMWLL8-071) in occlusal view.

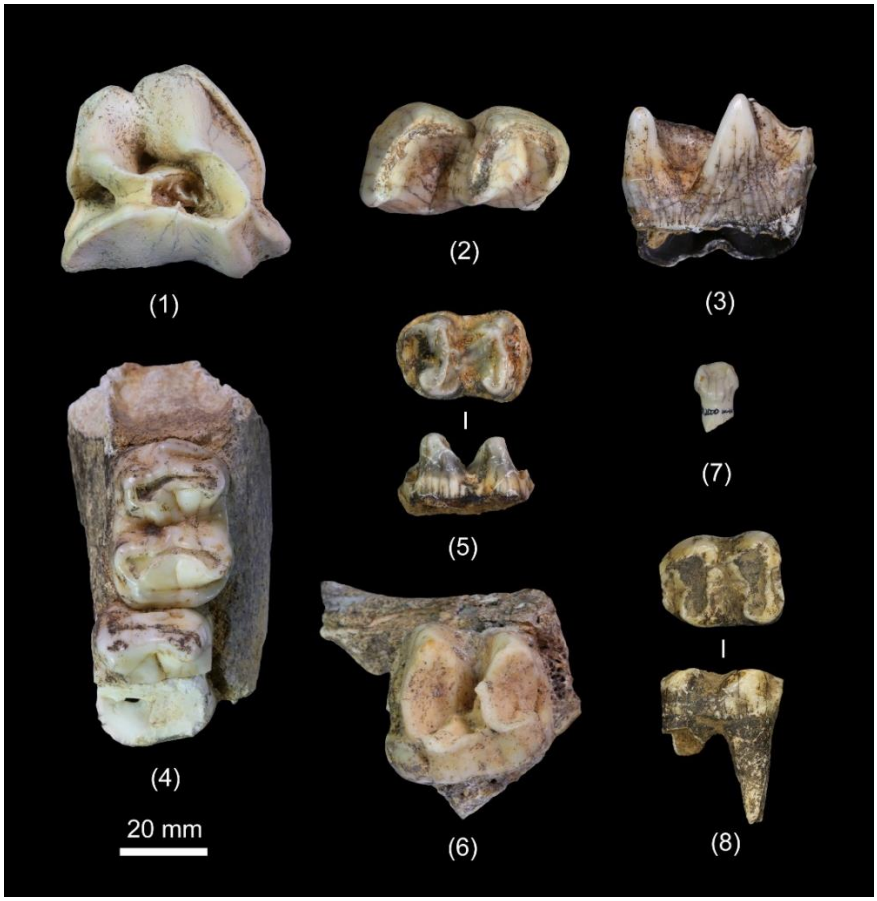

Fig. 7. Perissodactyla from Mocun cave. *Rhinoceros* sp.: (1) left M2 (PMWUL8-199) in occlusal view; (2) left m1 (PMWUL8-207) in occlusal view; (3) left m1 (PMWD-02) in lingual view. *Megatapirus augustus*: (4) right p4 and m1 (PMWD-135) in occlusal view; (5) right dp3 (PMWUL8-040) in occlusal and lingual view; (6) right M2 (PMWUL8-209) in occlusal view; (7) right I1 (PMWUL8-041) in lingual view; *Tapirus* cf. *sinensis*: (8) right p4 (PMWLL8-097) in occlusal and buccal view.

4.2.6. Artiodactyla

Sus scrofa: Among the Suids recorded at Mocun, the large pig *Sus scrofa* is represented by one hundred and twenty-three isolated teeth, covering all tooth types of the dentition. They were more frequent in L7. The dental pattern of the Mocun teeth is similar to that of *S. scrofa* from Yangjiawan cave 2 (Sun et al., 2021), which shows more complex occlusal folds on molars and more developed accessory tubercles and styles. The identifiable lower canines display the classic "scrofa" type, with a triangular cross-section with a lingual side wider than the buccal side, a high-crown and a thin enamel. *Sus scrofa* is recorded from the Middle Pleistocene in China. The range of dimensions is close to that of *S. scrofa* from Yenchingkuo, Tam Hang South in Laos and Duoi U'Oi in Vietnam (Colbert and Hooijer, 1953; Bacon et al., 2011, 2008) (Table 3-4) (Fig. 8).

Sus cf. *xiaozhu*: A fragmentary lower molar referred to *Sus xiaozhu* was ground-collected. This m1/m2 crown has a rectangular outline, and a highly worn and narrow anterior lobe. The four main cuspids are worn, but we can see a small accessory median cuspid. There are no accessory cuspids

in the valley, and the mesial margin of the crown is weakly developed. The morphology and size of the Mocun molar is close to *Sus xiaozhu* identified by Han et al. (1975) in the Bijiashan Cave, which is characterized by its small dimensions and simple occlusal pattern. The molar of Mocun is slightly smaller than those of Mohui Cave and *Giantopithecus* Cave, and its dimensions, the maximum residual width is 7.69 mm and the residual length is 9.48 mm, fall within the range of specimens from Jianshi and Bijiashan caves (Fig. 8). *Sus xiaozhu* was first discovered in the Early Pleistocene of China, and its latest appearance is in the Middle Pleistocene Hejiang cave (Zhang et al., 2014; Louys and Robert, 2020). However, during the survey of the Bubing basin, some remains of *S. xiaozhu* have also been recorded in Late Pleistocene to Holocene sites, but the data are not yet published (Wang, 2005). The discovery of the Mocun tooth would be an additional evidence that *S. xiaozhu* lived in the Late Pleistocene, but more comprehensive data are needed to confirm this statement.

Table 3-3. Dimensions of measurable Perissodactyla teeth from Mocun cave (mm).

Teeth	N	Length Range	x	Anterior Width Range	x	Posterior Width Range	x
Rhinoceros sp.							
DP1	2	24.34-27.99	26.17	18.96-22.29	20.63	19.88-23.34	21.61
DP3	3	30.04-37.5	33.84	29.46-36.95	32.58	29.17-35.05	31.59
dp2	4	28.13-31.97	30.25	13.44-14.63	14.06	14.7-16.62	15.93
dp3	2	42.24-43.39	42.82	17.19-18.71	17.95	20.13-20.53	20.33
P1	3	28.76-29.93	29.43	21.01-23.05	22	21.34-23.29	22.32
M2	1	/	50.85	/	47.85	/	42.21
p2	1	/	20.23	/	10.95	/	/
m1	2	42.41-42.82	42.62	19.28-20.91	20.1	22.11-23.25	22.68
m2	3	41.45-44	42.56	16.94-24.04	20.69	20.21-23.2	21.71
m3	1	/	49.12	/	22.26	/	22.15
Megatapirus augustus							
M2	1	/	33.14	/	33.74	/	28.28
dp3	1	/	30.89	/	20.42	/	21.27
dp4	2	/	33.23	19.43-22.24	20.84	19.29-19.74	19.52
p4	1	/	30	/	/	/	24.3
m1	1	/	33.11	/	24.71	/	22.93
m3	1	/	36.66	/	25.41	/	20.46
Tapirus cf. *sinensis*							
p4	1	/	26.74	/	20.5	/	20.95

Muntiacus reevesi: Eleven small teeth attributed to the small-sized Cervid *Muntiacus reevesi* have been recovered in L7 and L8. Some upper premolars, likely P2 or P3, display an entoflexus (a fold between the protocone and the hypocone) on the lingual side and a medial crista. A weak entostyle is present on upper molars. The morphology conforms to that of *M. reevesi* described in

the Yangjiawan and Fuyan caves (Zhang et al., 2018). The size of Mocun teeth falls within the range of fossil specimens, but is larger than that of the extant species. Based on their extremely small size, we also attributed three lower incisors to *M. reevesi* (Fig. 8).

Muntiacus muntjak: Sixty-four teeth, more numerous in L7 than in L8, also belonging to a small-sized cervid are referred to *Muntiacus muntjak*. Among these specimens, some upper premolars identified as P2 and P3 have an entoflexus on the lingual side. The others with no or weak entoflexus are identified as P4. The upper molars have developed mesostyle and metacone, and display an entostyle. The p4s show a "primitive" type with the metaconid separated from the paraconid. These dental patterns are consistent with *M. muntjak* described in Yixiantian cave (Pan, 2021), Yangjiawan and Fuyan cave (Zhang et al., 2018), and there is an overlap between populations from these sites and other Indochinese sites (Duoi U'Oi; Bacon et al., 2008) (Table 3-4, Fig. 8).

Rusa (*Cervus*) *unicolor*: This large-sized species of Cervid is represented by twenty-one specimens from L7 and L8. The teeth are large and robust and covered by a thick enamel. The upper premolars show the characteristics of the species with large lobes, protocone and hypocone, with a clear separation (entoflexus) between cusps on the lingual side. Cusps and styles are well-developed. In relation to lower premolars, we observed the molarization of the p4s, with the metaconid fused with the paraconid (Fig. 8).

Cervidae gen. et sp. indet.: In addition, eleven large teeth could not be accurately identified. These teeth are probably referred to different species.

Bos (*Bibos*) sp.: The L7, L8 and ground level produced thirteen teeth attributed to *Bos (Bibos)* sp., and consisting of lower milk teeth and permanent premolars and molars, including two upper molars in a fragmentary maxillary bone (Fig. 8). Overall, the teeth are massive, and the cusps and styles on molars are well-developed. On lower molars, the salient metastylid is close to the metaconid. On the basis of these characteristics, and despite the lack of p2, the most diagnostic tooth to identify *Bos* from *Bubalus*, the teeth are similar to Bos (*Bibos*) specimens described in Bailong cave and Sanhe cave (Wang et al., 2015; Dong et al., 2011), and are morphologically distinct from *Bubalus* and *Leptobos* (present in the Early Pleistocene of southern China). The dimensions of all of the Mocun teeth are comparable to those of fossils from Bailong cave and Yenchingkuo assigned to *Bibos gaurus grangeri* (Colbert and Hooijer, 1953). They are also comparable to scattered specimens from other southeast Asian sites, attributed to *Bibos gaurus* (e. g. Han, 1987; Zong, 1987; Huang and Fang, 1991), or *Bos sauveli* (Bacon et al., 2015, 2018b) (Table 3, Fig. 8).

Caprinae gen. et sp. indet.: Two cheek teeth of Caprine were respectively found in L7 and L8. The Mocun molar and premolar have a simple crescent shape with no accessory structure (crista, style or stylid), and a simple occlusal pattern. Based on these features, there is a possibility that these teeth belong to an Antilopinae. However, this taxon has not been recovered in Southern China during the Late Pleistocene. Therefore, we cautiously referred them to Caprinae gen. et sp. indet.

Table 3-4. Dimensions of measurable Artiodactyla teeth from Mocun cave (mm). MD, mesiodistal; BL, Buccolingual.

Teeth	N	Length (MD) Range	x	Width (BL) Range	x
Rusa (*Cervus*) *unicolor*					
P2	2	15.3-17.01	16.16	12.59-16.09	14.34
P4	1	/	15.24	/	20.63
M1	3	19.42-25.3	23	17.16-23.9	21.21
M2	1	/	20.9	/	19.34
M3	3	19.01-22.2	21.02	17.67-22.58	19.74
p2	1	/	15.25	/	11.38
p3	3	16-20.28	18.53	9.8-10.74	10.42
p4	2	17.71-21.28	19.5	10.82-12.21	11.52
m1	3	19.84-21.89	20.72	12.98-16.64	14.66
m3	1	/	34.02	/	14.92
Muntiacus muntjak					
P2	4	8.6-11.53	10.20	10.05-11.97	11.05
P3	7	8.68-11.7	10.23	8.85-13.82	11.26
P4	4	8.14-10.29	9.28	11.57-12.78	12.2
M1/2	14	10.31-14.75	12.29	11.34-16.58	14.3
M3	3	13.1-13.56	13.35	12.6-16.22	14.63
p2	7	7.83-9.3	8.72	4.59-5.47	5.02
p3	6	9.75-10.96	10.26	5.24-6.68	5.99
p4	3	10.42-12.81	11.45	6.72-7.18	7
m1/2	13	11.58-15.52	13.37	7.8-11.66	9.81
m3	3	18.68-19.55	19.03	9.37-10.18	9.71
Muntiacus reevesi					
P2	1	/	8.85	/	7.72
P3	2	6.61-6.69	6.65	8.67-9.41	9.04
M2	1	/	9.66	/	10.77
M3	2	8.45~9.62	9.03	9.44~11.84	10.64
p3	1	/	7.46	/	5.04
m1	1	/	10.11	/	7.28
Bos (*Bibos*) sp.					
M1	1	/	27.05	/	30.34
p3	1	/	22.85	/	11.1
p4	2	22.42-23.3	22.86	16.04-16.85	16.45
m1/2	5	30.04-34.68	32.41	18.12-22.47	20.02
m3	3	45.93-48.48	47.51	20.29-22.94	22.05
Sus scrofa					
P2	2	13.49-13.51	13.5	9.46-9.55	9.51
P3	7	11.57-18.53	13.98	8.94-12.82	10.91
P4	10	11.79-15.24	13.57	11.98-16.45	14.54
M1	14	16.17-19.35	17.6	13.36-16.74	15.2
M2	6	20.5-25.07	23.02	17.66-20.15	18.82
M3	6	33.31-43.47	37.75	19.49-25.08	22.03
p2	2	10.4-12.35	11.38	5.73-6.13	5.93
p3	6	14.63-16.02	15.06	7.76-11.08	9.39
p4	7	14-16.78	15.98	10.36-12.02	11.11
m1	16	14.53-19.9	17.82	11.51-13.67	12.47
m2	14	20.19-26.94	23.98	13.91-18.03	16.11
m3	10	36.34-45.47	41.2	15.8-19.96	17.76

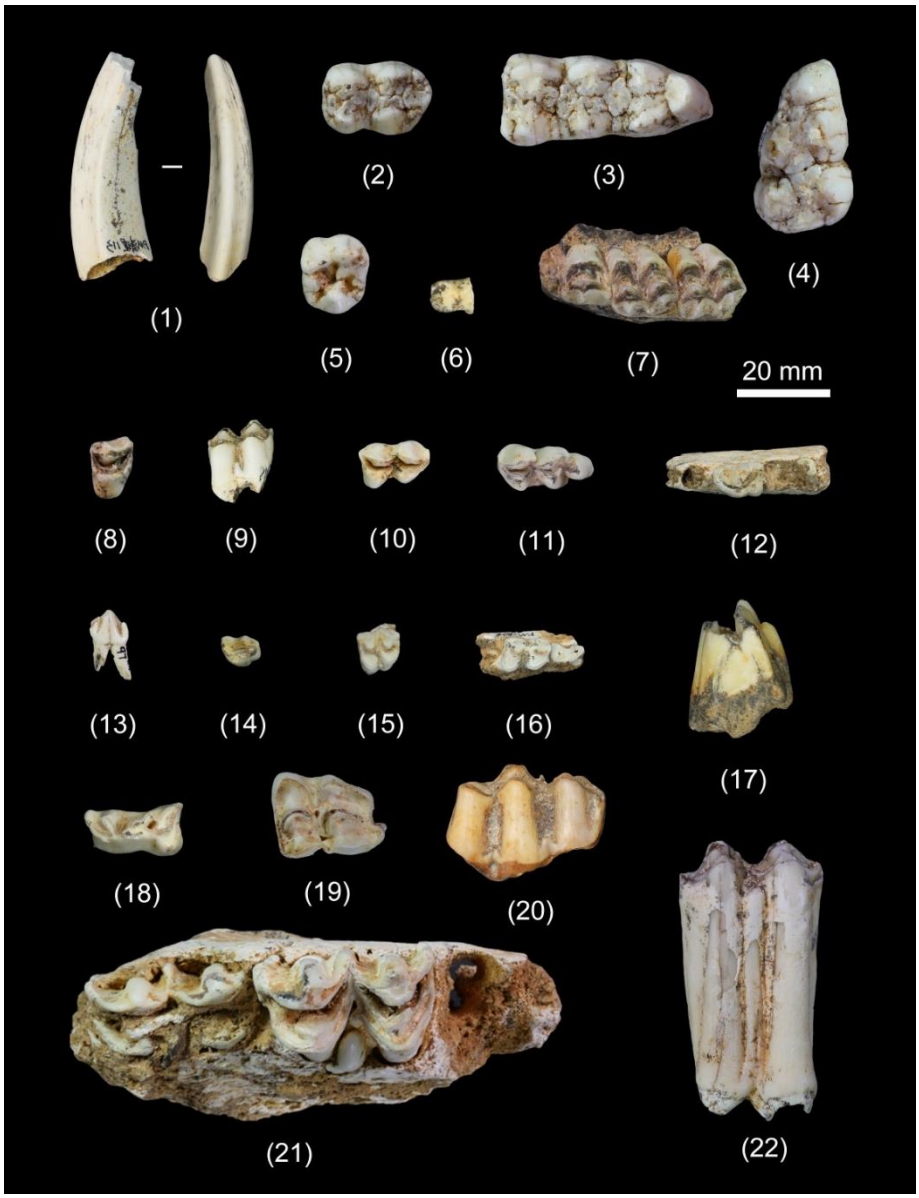

Fig. 8. Artiodactyla from Mocun cave. *Sus scrofa*: (1) right lower canine in buccal and anterior view (PMWD-113); (2) left m2 (PMWUL8-002) in occlusal view; (3) left m3 (PMWD-99) in occlusal view; (4) left M3 (PMWD-100) in occlusal view; (5) right P4 (PMWUL8-163) in occlusal view. *Sus xiaozhu*: (6) lower molar (PMWD-163) in occlusal view; *Muntiacus muntjak*: (7) left P4, M1 and M2 (PMWD-27) in occlusal view; (8) right P3 (PMWLL8-073) in occlusal view; (9) right m1/m2 (PMWUL8-072) in buccal view; (10) right m1/m2 (PMWUL8-047) in occlusal view; (11) right m3 (PMWD-81) in occlusal view; (12) left p4 (PMWD-85) in occlusal view. *Muntiacus reevesi*: (13) left p2 (PMWD-97) in lingual view; (14) right P2 (PMWUL8-054) in occlusal view; (15) left M1/M2 (PMWLL8-015) in occlusal view; (16) right m1 (PMWD-94) in occlusal view. *Rusa* (*Cervus*) *unicolor*: (17) left M1 (PMWD-70) in mesial view; (18) right p3 (PMWD-75) in occlusal view; (19) right M3 (PMWD-11) in occlusal view; (20) right m3 (PMWD-12) in buccal view. *Bos* (*Bibos*) sp.: (21) left M1 and M2 (PMWLL8-005) in occlusal view; (22) left m1/m2 (PMWD-64) in buccal view.

4.3. Taphonomic processes

In the stratigraphical sequence, the deposits L7 and L8 are the most fossiliferous. The thick sediment indicates a long-term process of fossil accumulation. The composition of the mammalian fauna (Table S15) and the size variation of taxa (Tables S1-14) differ little between L7 and L8, that suggests a unified faunal assemblage. We note however some differences in the proportions of specimens by taxonomic group in the different layers. For example, using NISP, the proportion of Primates (predominantly Cercopithecidae) is relatively large in L8 (44%), and much smaller in L7 (4.8%). In relation to Artiodactyla, NISP appears prominent in L7 with 53.2% of specimens and only 26.4% in L8 (Table 4).

Using Fisher's exact test on the distribution ratio of NISP of the six mammalian Orders in L7 and L8, at 95% confidence interval, the p-values show significant statistical differences between both layers (Table 4). These differences can be influenced by a variety of factors during the accumulation, transport and deposition of remains. However, they are difficult to explain because, overall, both fossiliferous deposits share similar characteristics: 1) carnivores are present in both layers; 2) small- to large-sized mammalian fossils are similarly preserved; and 3) specimens, mostly isolated teeth and few bone fragments without any complete long bones, show a similar taphonomic pattern with either gnawed or rounded marks (Fig. 9).

The carnivores recorded at Mocun (spotted hyena and small felid) may have played a role in the accumulation process prior to porcupines. Because of the small sample size using MNIf by taxon in the different layers, we analysed the MNIc by combining data from the ground, L7 and L8. In Artiodactyla, data of cervids (MNIc = 20, 15 adults, 5 young adults), suids (MNIc = 18, 12 adults and 6 young adults), and bovids (MNIc = 6, 4 adults, 1 young adult and 1 juvenile) indicate the absence or the rarity of juveniles. These results clearly show a bias toward adult individuals (that differs from the catastrophic mortality pattern (L-shaped) in which all age categories are represented). Abundant small-sized rodents being also preserved, the action of destructive water flows can't only explain the lack of light and fragile milk teeth of these large animals. Moreover, human fossils or artefacts are absent at Mocun and in the surrounding area, and there is no evidence of human activities in the site.

Compared to these taxa, the rhinos provide an unexpected high proportion of young individuals (MNIc = 11), with 6 juveniles and 4 young adults, and only one adult individual. The juvenile-dominant structure differs from that of natural populations, probably biased by the predation or other biotic factors. This pattern, also present in the Late Pleistocene Nam Lot cave in Laos (86-72 ka), has been associated to the pack hunting behavior of hyenas able to kill calves of rhinoceros up to ~400 kg (Bacon et al., 2015).

Table 4. The number of identifiable specimen (NISP) and minimum number of individuals (MNI) from the different layers of Mocun cave

Order	Subfamily/family	NISP/NISP%			MNIf			MNIc		
		ground/%	L7/%	L8/%	ground	L7	L8	ground	L7	L8
Primates	Cercopithecidae	9/5.5	9/4.8	81/42.0	4A	3A	14A	3A, 1YA	3A, 1YA	13A, 1YA
	Homininae			1/0.5			1A			
	Hylobatidae			2/1.0			1A			
Rodentia	Hystricidae	17/10.4	38/20.3	36/18.8	5A	9A	5A			
Proboscidae	Stegodontidae	5/3.1	2/1.1	1/0.5	2A	1A, 1J	1J			
	Elephantidae	4/2.5	1/0.5	1/0.5	1A, 2J	1A	1A			
Carnivora	Canidae	2/1.2	2/1.1		1A	1A				
	Ursidae	6/3.7	11/5.9	1/0.5	2A	2A	1A			
	Ailuropodidae	1/0.6	1/0.5		1A	1A				
	Hyaenidae	1/0.6		1/0.5	1A		1A	1YA		1A
	Others	7/4.3	7/3.7	9/4.7	6A	5A	5A			
Perissodactyla	Rhinocerotidae	12/7.4	13/7.0	6/3.1	2A, 2J	1A, 1J	1A, 1J	2YA, 2J	1A, 3J	1J, 2YA
	Tapiridae	4/2.5	4/2.1	1/0.5	1A, 1J	1A, 1J	1A			
Artiodactyla	Suidae	36/22.1	56/29.9	31/16.1	5A	5A	5A	4A, 1YA	5A, 3YA	3A, 2YA
	Cervidae	51/31.3	38/20.3	18/9.4	5A	7A	4A	5A, 3YA	7A, 1YA	3A, 1YA
	Bovidae	8/4.9	4/2.1	1/0.5	2A, 1J	1A	1A	2A, 1J	1A, 1YA	1A
	Caprinae		1/0.5	1/0.5		1A	1J			
Total		**163/100.0**	**187/100.0**	**192/100.0**						

Fisher's exact test (confidence level=0.95) **p-value = 0.0004998**

Table 5 illustrates the proportion of teeth in different groups showing gnawing marks on roots, from the ground level, L7 and L8. The results indicate a similar taphonomy. The Cercopithecidae from L7 and L8 display 30.8% and 29.8% of teeth with gnawed roots, respectively; in Ursidae, the gnawed roots account for 72.7% and 0% (only one specimen); 53.6% and 38.7% in Suidae; and 26.3% and 37.5% in Cervidae. The dimensions and patterns of the grooves on roots of teeth or bones match with the size of incisors of porcupines as shown in Figure 9, indicating intense activities of these large rodents to collect remains and accumulate bones and teeth from carcasses left at the site. We note also gnawing marks of small-sized rodents, like Rhizomyidae or Muridae recorded in the assemblage of micromammals from Mocun cave. The data clearly indicate that rodents were the last accumulator agents before burial, and particularly porcupines widespread in the region. Indeed, gnawed marks caused by rodents are generally observed in most Pleistocene mammalian assemblages from karstic caves in Southern China and mainland Southeast Asia (e. g. Pei, 1938; de Vos and Long, 1993; Long et al., 1996; Bacon et al., 2004, 2006, 2015).

Interestingly, some of the fossils also present other modifications, like crowns with rounded or blunted surfaces caused by water, indicating that the deposits in cave were transported by flowing waters for a long period (Fig. 9). The water circulation is supposed to be the major agent of transport, selection and deposition of remains across the karstic fissures and galleries (Duringer et al., 2012). At Mocun, the preservation in the west part of the cave of large mammalian fossils, along with a plenty of smaller rodent fossils, suggests that the water flows could have been variably powerful, due to various energy environments, or that it was not a completely open water condition. Moreover, the presence of larger bones such as the nearly complete skeleton of an elephant in the cave in a different layer also suggests a different taphonomic history in the east part of the cave, with animals most likely dropped and trapped in the cavities.

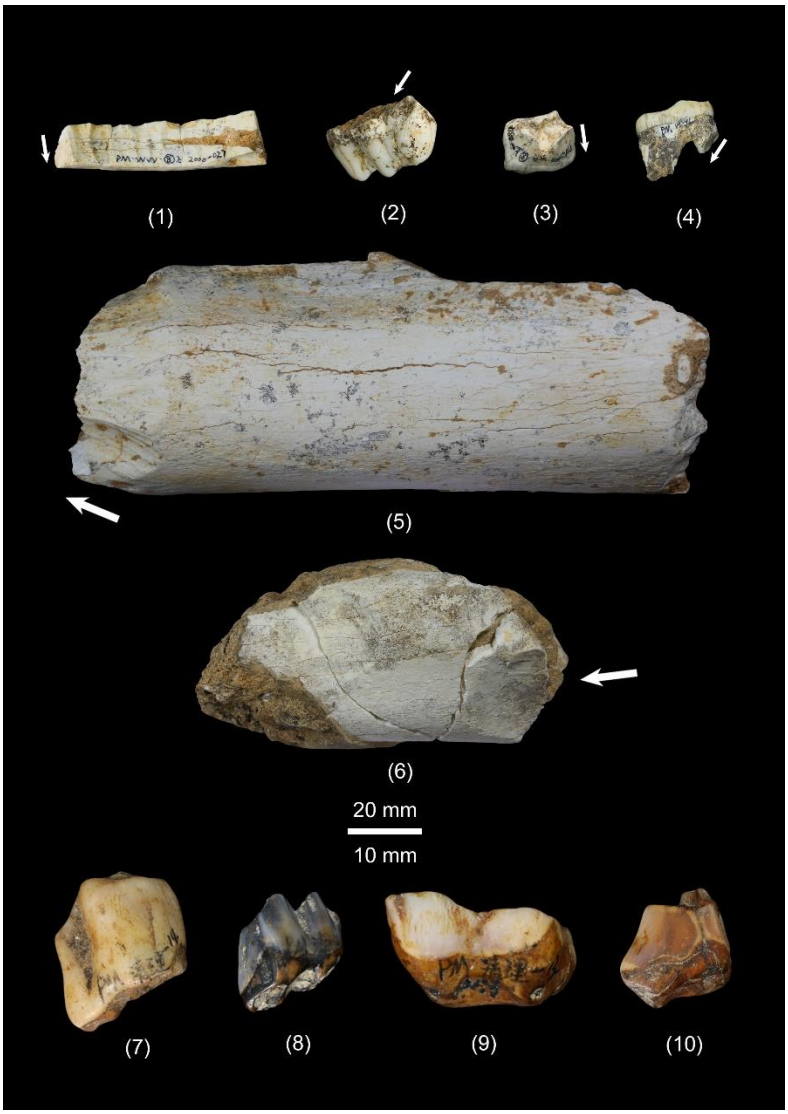

Fig. 9. Different marks observed on remains. (1-6) Gnawing marks on teeth and bones; (7-10) Rounding marks on crowns.

5. Discussion

5.1. Composition of the Mocun fauna and position in the evolutionary sequence

The Mocun fauna consists of 25 identified taxa belonging to six orders (Primates, Rodentia, Proboscidea, Carnivora, Perissodactyla, and Artiodactyla), most of which are modern species still living in the island and mainland Asia, whereas some are archaic species typical of the "*Stegodon-Ailuropoda*" faunas in southern China (*Stegodon orientalis*, *Crocuta ultima*, *Megatapirus augustus*, *Tapirus sinensis*, *Sus xiaozhu* and *Hystrix magna*), with species like *H. magna* and *S. xiaozhu* recorded in the region since the Early Pleistocene (Norton et al., 2010).

By compiling data on the global and local extinctions (absence of taxa due to changes in distribution ranges) (Tables 1-4), extinct species at Mocun accounted for about 40%. Moreover, when we simply calculate the proportion of extinct taxa in Asia, either genera or species, the results highlight that the Mocun fauna was a mixed fauna with with 24% (6 out of 25) of species now extinct, along with a high proportion of modern species, like the other mammalian communities in the region, Zhiren cave (25 %, 5 out of 20) or Fuyan cave (13.6%, 3 out of 22) (Jin et al., 2009; Li et al., 2013) (Tables 1-4). The proportion of extinct taxa was slightly higher for the late Middle Pleistocene faunas from the region, as show the earliest Heijiang cave (35.2%, 6 out of 17) or Ganxian cave (30%, 6 out of 20). The estimated age range of the Mocun faunal deposits in L7 and L8 between 66 and 86 ka, with a maximum age of 101 ka at the base of the sequence, represents a period from the interglacial MIS5 (130-71 ka; Lisiecki and Raymo, 2005) to the transitional glacial stage MIS 5-4 (MIS4, 71-47 ka), and its composition compared with that of late Middle Pleistocene local faunas, still shows a wide overlap.

Furthermore, compared with island and mainland southeast Asian records, it seems that southern China retained more archaic elements over the period, as indicated by the late Middle Pleistocene data of Coc Muoi in northern Vietnam (10%, 2 out of 20), Punung in Java (0%), Ngalau Gupin in Sumatra (4%, 1 out of 22), and the Late Pleistocene data of Nam Lot (10%, 2 out of 20) in northern Laos, and Duoi U'Oi (0%) in northern Vietnam (Tables 3-4).

It has been suggested that the replacement of *Stegodon* by *Elephas*, and the predominance of this modern genus in the Late Pleistocene sites (Li et al., 2013; Jin et al., 2009), was a criteria to distinguish the Middle Pleistocene *Stegodon-Ailuropoda* faunal association from the Late Pleistocene *Elephas-Megatapirus* faunal association. Indeed, in the Zhiren fossiliferous deposits initially dated to 116-106 ka (Liu et al., 2010), *Elephas maximus* represents a significantly high proportion of specimens in the fauna. However, the age range of the Zhiren cave was recently questioned to be in the late Middle Pleistocene (190-130 ka; Ge et al., 2020). Therefore, the reliable dating and abundant fossil materials of the Mocun site, with the co-occurrence of both *Stegodon* and *Elephas*, provide essential information on the composition of mammalian communities in the first half of the Late Pleistocene, and fill in the blank of researches in southeast Guangxi, for the succession of faunas from the Middle Pleistocene to the Late Pleistocene. These data also support that both lineages, *S. orientalis* and *E. maximus*, were present in a vast zone in Indochina during this period, as show the faunal records of Coc Muoi (147-118 ka) in northern Vietnam and Nam Lot (86-72 ka) in northern Laos (Bacon et al., 2015). It also offers perspectives for further comparative studies with mainland Southeast Asia sites from the same period.

There is no difference in the faunal composition of the layers (ground, L7, L8) (Table S15), but the proportion of some specimens by taxon (NISP) differs remarkably. This is the case of primates and artiodactyls. While arboreal monkeys (mainly cercopithecid) dominated in L8, ground-dwelling artiodactyls (cervid, bovid, and suid) did in L7. The abundance of both groups indicates a forest-dominated habitat. Furthermore, we observe some variation in the occurrence of the two species of tapirs, the larger *M. augustus* present in L7 replacing the smaller *T. sinensis* in L8 (Fig. 10). Taphonomic processes can disturb the conservation of fossils, generally based on size (small *vs* large; fragmentary *vs* complete) and property (bone *vs* tooth, deciduous *vs* permanent tooth). However, natural deposition agents do not separate species whose teeth are in the same size range. Therefore, the changes might represent a transition between two successive periods. Nevertheless, this observation is based on a small sample size, and it remains difficult to say if this variation reflects changes either in environments in mid-Late Pleistocene with a vegetation that would have favored the abundance of large ungulates, or in prey choice by carnivores, or if it could be due to taphonomic biases. The environmental transition in the end of the last interglacial period requires further researches.

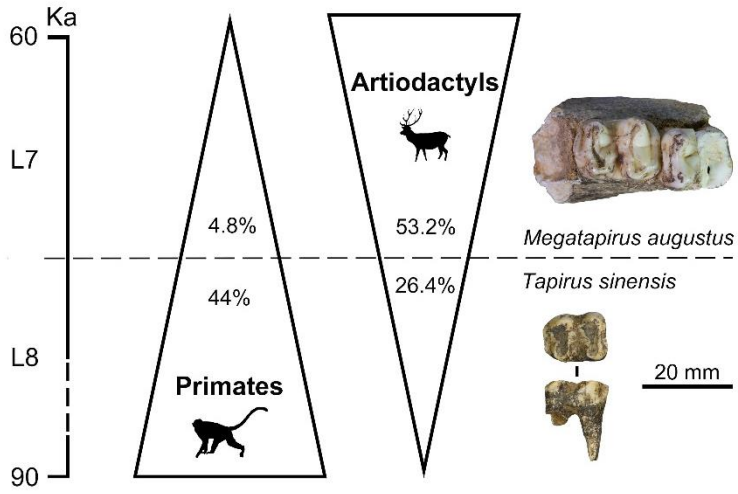

Fig. 10. Main differences observed between L7 and L8: Quantitative representation of primates *vs* artiodactyls and occurrence of tapirs.

5.2. Palaeoecology of the "Stegodon-Ailuropoda" fauna

During the Pleistocene, a mixture of vegetation types coexisted in mainland southeast Asia, some providing areas of refugia for the long-term survival of species (Suraprasit et al., 2018, 2020). The gradual change to colder and/or wetter conditions from the Early Pleistocene to the Late Pleistocene in the region most likely contributed to the decline of some species with particular foraging strategy, such as *Gigantopithecus blacki* (Sun et al., 2019; Hu et al., 2022).

Using carbon and oxygen isotope records from the mainland southeast Asia (southern China

and Indochinese subregion), Louys and Roberts (2020) proposed that during the Middle Pleistocene, the mainland was covered predominantly by savannahs, later replaced by closed-canopy forests in the Late Pleistocene. While the center of the Indochinese peninsula remained covered by open habitats, Southern China is regarded at the transition between the late Middle to the Late Pleistocene, as a closed and homogeneous environment, all results indicating C_3-dominated habitats (inhabited by *Gigantopithecus*, *Elephas*, *Ailuropoda*), with mixed C_3-C_4 and C_4 areas with grasses (Zhao and Zhang, 2013; Nelson, 2014; Ma et al., 2017; Stacklyn et al.,2017; Sun et al., 2019). Bacon et al. (2021) further demonstrated that the return of these rainforest conditions in the region occurred ~130 ka, due to a major cooling event at the end of MIS 6, with a notable drop of monsoon intensity (Wang et al., 2008).

The Mocun fauna (66-101 ka) suggests a predominantly forested environment in the first half of the Late Pleistocene, as observed in ecosystems of Laos and Vietnam located at the same latitudes. It contains a large number of tropical and subtropical forest-dwelling species (e. g. *Macaca, Sus, Muntiacus,* etc.), some specifically adapted to lowland canopy forests (e. g. *Pongo*, *Rhinoceros*, *Tapirus, Megatapirus*, *Stegodon*), and some others (e. g. *Rusa*, *Bos,* or caprinae) able to live in more open habitats, suggesting a diversified ecosystem. We note however the absence at Mocun of cervids of medium size, most of them being mixed-feeders or exclusive grazers in savannahs and grasslands habitats (Suraprasit et al. 2018, 2020).

In comparison with other Late Pleistocene sites of the region, more archaic species survived in Mocun (like *S. xiaozhu* or *H*. *magma*), a longevity possibly related to the unique geographical location of the site (latitudinal conditions, temperature, degree of moisture etc.). By contrast, the Indochinese peninsula harbored modern species (*S. scrofa, S. barbatus*, *H. brachyura*) at the same time. The geological context may have been also important. Most of mammalian faunas were found in karstic caves of Bubing basin and Chongzuo. The southeast of Guangxi, where the Mocun cave is located, is dominated by broad plains and granite hills, representing a habitat different from the limestone mountains.

Our results demonstrate that the mammalian "*Ailuropoda-Stegodon*" faunas from Southern China preserved during the first half of the Late Pleistocene a great biodiversity of large-bodied herbivores, most likely due to the great carrying capacity of the rainforest ecosystems along with the geological context. To this respect, the region was most likely an important reserve of biodiversity for species adapted to rainforest conditions. Bacon et al. (2021) hypothesized that canopy forest-dwelling species from southern China might have expanded to lower latitudes in the face of the cooling event in mid-Late Pleistocene ~70 ka. This dispersal was selective, due to different responses of species to environmental shifts, that renewed the composition of mammalian communities over the period (Jablonski and Sepkoski, 1996; Stewart, 2009).

6. Conclusion

The thick and complete deposits in Mocun cave represents a long period of accumulation. Based on the analysis of fossil evidence in the richest layers L7 and L8, we evaluated two main taphonomic agents, water flows and rodents. The age of fossil-bearing layers L7 and L8 (66-86 ka), the relative abundance of some groups (cercopithecid *vs* cervid), and the occurrence of some taxa (tapirid), reflect changes in the fauna. These differences in the composition between both layers

might be the result of different taphonomic processes, or due to environmental changes in mid-Late Pleistocene. Finally, the Mocun faunal assemblage with accurate dating shows the difficulty in distinguishing late Middle from Late Pleistocene "*Ailuropoda-Stegodon*" mammalian faunas only based on their composition.

Author statement

Yaobin Fan (Institute of Culture Heritage, Shandong University, Qingdao, 266 237, China; fanyaobin11@mail.sdu.edu.cn): identifying and measuring fossil materials, responsible for statistic analysis and figures and tables production, the main author to write this paper. Qingfeng Shao (School of Geography, Nanjing Normal University, Nanjing, 210023, China; qingfengshao@njnu.edu.cn): conducting U-series dating experiment. Anne-Marie Bacon (UMR 8045 BABEL, CNRS, Universite de Paris, Faculté de Chirurgie dentaire, 1 rue Maurice Arnoux, 92 120 Montrouge, France; anne-marie.bacon@u-paris.fr): guiding paper revision and contribute to the part of method and discussion. Wei Liao (Institute of Culture Heritage, Shandong University, Qingdao, 266 237, China; liaowei@ sdu.edu.cn): identifying teeth fossils and executing preexperimental treatment. Wei Wang (Institute of Culture Heritage, Shandong University, Qingdao, 266 237, China; wangw@sdu.edu.cn): In charge of cave excavation, the part of stratigraphic description and guiding paper writing.

Declaration of competing interest

The authors declare that they have no known competing financial interests or personal relationships that could have appeared to influence the work reported in this paper.

Data availability

Data will be made available on request.

Acknowledgements

We thank Mr. Chenghan Lu, director of Pubei County Museum, and Mr. Chaolin Huang and Mr. Shichu Zhou of Natural History Museum in Guangxi for their participation on this rescue excavation in 2000. We also thank local villagers in Mocun for their kind assistance during our field work. This work has been supported by the Major Program of National Social Science Foundation of China (20&ZD246), the National Natural Science Foundation of China (41962003 and 42002025), the BaGui Scholars Project of the Guangxi Zhuang Autonomous Region, and the Open Fund of Key Laboratory of Environment Change and Resources Use in Beibu Gulf, Ministry of Education.

Table 5. Frequency of teeth by family and the proportion of gnawing marks on teeth.

	Cercopithecidae				Ursidae				Suidae				Cervidae			
	ground	**L7**	**L8**	**Total**	**ground**	**L7**	**L8**	**Total**	**ground**	**L7**	**L8**	**Total**	**ground**	**L7**	**L8**	**Total**
Frequency (Upper/Lower)	4/5	5/4	56/25	65/34	4/2	6/5	0/1	10/7	15/21	26/30	12/19	53/70	24/26	17/21	12/5	53/52
Frequency (Deciduous/Permanent)	0/9	0/9	0/81	0/99	0/6	0/11	0/1	0/18	0/36	0/56	0/31	0/123	0/50	0/38	0/17	0/105
Percentage (ungnawed root)	50.0%	69.2%	70.2%	68.2%	80.0%	27.3%	100.0%	47.1%	58.3%	46.4%	61.3%	53.7%	70.0%	73.7%	62.5%	69.5%
Percentage (gnawed root)	50.0%	30.8%	29.8%	31.8%	20.0%	72.7%	0.0%	52.9%	41.7%	53.6%	38.7%	46.3%	30.0%	26.3%	37.5%	30.5%

References

Bacon, A.-M., Demeter, F., Schuster, M., Long, V.T., Thuy, N.K., Antoine, P.-O., Sen, S., Nga, H.H., Huong, N.M., 2004. The Pleistocene Ma U'Oi cave, northern Vietnam: Palaeontology, sedimentology and palaeoenvironments. Geobios 37(3), 305–314.

Bacon, A.-M., Demeter, F., Roussé, S., Long, V.T., Duringer, P., Antoine, P.-O., Thuy, N.K., Huong, N.M., Dodo, Y., Matsumura, H., Schuster, M., Anezaki, T., 2006. New palaeontological assemblage, sedimentological and chronological data from the Pleistocene Ma U'Oi cave (Northern Vietnam). Palaeogeogr. Palaeoclimatol. Palaeoecol. 23, 280–298.

Bacon, A.M., Demeter, F., Duringer, P., Helm, C., Bano, M., Long, V.T., Thuy, N.T.K., Antoine, P.-O., Mai, B.T., Huong, N.T.M., Dodo, Y., 2008. The Late Pleistocene Duoi U'Oi cave in northern Vietnam: palaeontology, sedimentology, taphonomy and palaeoenvironments. Quat. Sci. Rev. 27, 1627–1654.

Bacon, A.-M., Duringer, P., Antoine, P.-O., Demeter, F., Shackelford, L., Sayavongkhamdy, T., Sichanthongtip, P., Khamdalavong, P., Nokhamaomphu, S., Sysuphanh, V., Patole-Edoumba, E., Chabaux, F., Pelt, E., 2011. The Middle Pleistocene mammalian fauna from Tam Hang karstic deposit, northern Laos: new data and evolutionary hypothesis. Quat. Int. 245, 315–332.

Bacon, A.-M., Westaway, K., Antoine, P.-O., Duringer, P., Blin, A., Demeter, F., Ponche, J.-L., Zhao, J.-X., Barnes, L.M., Sayavonkhamdy, T., Thuy, N.T.K., Long, V. T., Patole-Edoumba, E., Shackelford, L., 2015. Late Pleistocene mammalian assemblages of Southeast Asia: New dating, mortality profiles and evolution of the predator–prey relationships in an environmental context. Palaeogeogr. Palaeoclimatol. Palaeoecol. 422, 101–127.

Bacon, A.-M., Duringer, P., Westaway, K., Joannes-Boyau, R., Zhao, J., Bourgon, N., Dufour, E., Pheng, S., Tep, S., Ponche, J.-L., Barnes, L., Blin, A., Patole-Edoumba, E., Demeter, F., 2018a. Testing the savannah corridor hypothesis during MIS2: The Boh Dambang hyena site in southern Cambodia. Quat. Int. 464, 417–439.

Bacon, A.-M., Antoine, P.-O., Huong, N.T.M., Westaway, K., Tuan, N.A., Duringer, P., Zhao, J., Ponche, J.-L., Dung, S.C., Nghia, T.H., Minh, T.T., Son, P.T., Boyon, M., Thuy, N.T.K., Blin, A., Demeter, F., 2018b. A rhinocerotid-dominated megafauna at the MIS6-5 transition: The late Middle Pleistocene Coc Muoi assemblage, Lang Son province, Vietnam. Quat. Sci. Rev. 186, 123–141.

Bacon, A.-M., Bourgon, N., Dufour, E., Zanolli, C., Duringer, P., Ponche, J.-L., Antoine, P.-O., Shackelford, L., Huong, N.T.M., Sayavonkhamdy, T., Patole-Edoumba, E., Demeter, F., 2018c. Nam Lot (MIS 5) and Duoi U'Oi (MIS 4) Southeast Asian sites revisited: Zooarchaeological and isotopic evidences. Palaeogeogr. Palaeoclimatol. Palaeoecol. 512, 132–144.

Bacon, A.-M., Bourgon, N., Welker, F., Cappellini, E., Fiorillo, D., Tombret, O., Huong, N.T.M., Tuan, N.A., Sayavonkhamdy, T., Souksavatdy, V., Sichanthongtip, P., Antoine, P.-O., Duringer, P., Ponche, J.-L., Westaway, K., Joannes-Boyau, R., Boesch, Q., Suzzoni, E., Frangeul, S., Patole-Edoumba, E., Zachwieja, A., Shackelford, L., Demeter, F., Hublin, J.J., Dufour, E., 2021. A multi-proxy approach to exploring *Homo sapiens*' arrival, environments and adaptations in Southeast Asia. Sci. Rep. 11(1), 1–14.

Beden, M., Guerin, C., 1973. Le gisement de vertébrés du Phnom Loang (Province de Kampot, Cambodge). Faune du Pléistocène moyen terminal (Loangien). Travaux et Documents de

l'ORSTOM, Paris, pp. 27–97.
Brain, C.K., 1981. The hunters or the hunted? The University of Chicago Press, Chicago
Cai, Y., Qiang, X., Wang, X., Jin, C., Wang, Y., Zhang, Y., Trinkaus, E., An, Z., 2017. The age of human remains and associated fauna from Zhiren Cave in Guangxi, southern China. Quat. Int. 434, 84–91.
Chabaux, F., Riotte, J., Dequincey, O., 2003. U-Th-Ra fractionation during weathering and river transport, in: Bourdon, B., Henderson, G.M., Lundstrom, C.C., Turner, S.P. (Eds), Uranium-series Geochemistry. Reviews in Mineralogy and Geochemistry. Geochemical Society - Mineralogical Society of America, Washington, pp. 533–576.
Chen, S.K., Huang, W.P., Pei, J., He, C.D., Qin, L., Wei, G.B., Leng, J., 2012. The latest Pleistocene *Stephanorhinus kirchbergensis* from the Three Gorges area and re-evaluation of Pleistocene rhinos in Southern China. Acta Anthropol. Sin. 31, 381–394.
Colbert, E.H., 1943. Pleistocene vertebrates collected in Burma by the American Southeast Asiatic expedition. Trans. Am. Phil. Soc. 32, 395–429.
Colbert, E.H., Hooijer, D.A., 1953. Pleistocene mammals from the limestone fissures of Szechwan, China. Bull. Am. Mus. Nat. Hist. 102, 1–134.
Corbet, G.B., Hill, J.E., 1992. The mammals of the Indomalayan region. Natural History Museum Publications. Oxford University Press.
Dong W., Pan W., Sun C., Xu Q., Qin D., Wang Y., 2011. Early Pleistocene Ruminants from the Sanhe Cave, Chongzuo, Guangxi, South China. Acta Anthropol. Sin. 30(2), 192–205.
Duringer, P., Bacon, A.-M., Sayavongkhamdy, T., Thuy, N.T.K., 2012. Karst development, breccias history, and mammalian assemblages in Southeast Asia: A brief review. C. R. Palevol 11, 133–157.
de Terra, H., 1938. Preliminary report on recent geological and archaeological discoveries relating to early man in Southest Asia. Proc. Natl. Acad. Sci. 24, 407–413.
de Vos, J., Long, V.T., 1993. Systematic discussion of the Lang Trang fauna. Unpublished Report.
Edwards, R.L., Gallup, C.D., Cheng, H., 2003. Uranium-series dating of marine and lacustrine carbonates. Rev. Mineral. Geochem. 52, 363–405.
Erdbrink, D.P., 1953. A review of fossil and recent bears of the old world. Thesis of University of Utrecht.Fooden, J., 1990. The bear macaque *Macaca arctoides*: A systematic review. J. Hum. Evol. 19, 607–686.
Frisch, J.E., 1965. Trends in the evolution of the Hominoid dentition. Biblthca Primatol. Fasc. 3, pp. 130.
Fromaget, J., 1936. Sur la stratigraphie des formations récentes de la Chaine annamitique septentrionale et sur l'existence de l'Homme dans le Quaternaire inférieur de cette partie de l'Indochine. C. R. Acad. Sci., Paris 203, 738–741.
Ge, J.Y., Deng, C., Wang, Y., Shao, Q., Zhou, X., Xing, S., Pang, H., Jin, C., 2020. Climate-influenced cave deposition and human occupation during the Pleistocene in Zhiren Cave, southwest China. Quat. Int. 559, 14–23.
Guangxi Bureau of Geology and Mineral Resources, 1985. Regional geology of Guangxi Zhuang Autonomous Region. Geological Publishing, Beijing.
Guo, J., 1997. Note on a fossil skull of *Hystrix magna* Pei, 1987 (Rodentia, Mammalia) from Chongzuo, Guangxi. Vertebr. PalAsiat. 35(2), 145–153.
Han, D., Xu, C., Yi, G., 1975. Quaternary mammal fossils from Bijiashan, Liuzhou, Guangxi. Vertebr.

PalAsiat. 13(4), 250–256.
Han, D.-F., 1987. Artiodactyla fossils from Liucheng *Gigantopithecus* cave in Guangxi. Mem. Inst. Vertebr. Paleontol. Paleoanthropol. Acad. Sinica 18, 135–208 (in Chinese with English abstract).
Han, D.F., Xu, C.H., 1985. Pleistocene mammalian faunas of China, in: Rukang, W., Olsen, J.W. (Eds), Palaeoanthropology and Palaeolithic Archaeology in the People's Republic of China. Academic Press, New York, pp. 267–286 (in Chinese).
Hodgson, B.H., 1837. Description of the Gauri Gai (*Bibos subhemachalus*) of the Nepal forest. J. Asiat. Soc. Bengal 6, 499.
Hu, C., Qi, T., 1978. Gongwangling Pleistocene Mammalian Fauna of Lantian, Shaanxi. Science Press, Beijing.
Hu, Y., Jiang, Q., Liu F. et al., 2022. Calcium isotope ecology of early *Gigantopithecus blacki* (∼2 Ma) in South China. Earth Planet. Sci. Lett. 584, 1-9.Huang, W., 1979. On the age of the Cave-faunas of South China. Vertebr. PalAsiat. 04, 327–343.
Huang, W., Fang, Q., 1991. Wushan Hominid Site. China Ocean Press, Beijing.
Jablonski, D., Sepkoski, J. J., 1996. Paleobiology, community ecology and scales of ecological patterns. Ecology 77, 1367–1378.
Ji, H., 1977. Division of Quaternary Mammalian Fauna in South China. Vertebr. PalAsiat. 04, 271–277.
Jiangzuo, Q., Zhang, B., Deng, L., Chen, X., Wen, J., Tong, H., 2018. Fossil carnivora (Mammalia) from Yangjiawan Cave 2, Pingxiang, Jiangxi, with remarks about the tooth identification of Quaternary Carnivores, in: Dong Wei (Ed), Proceedings of the Sixteenth Annual Meeting of the Chinese Society of Vertebrate Paleontology. China Ocean Press, Bejjing, pp. 119–146 (in Chinese).
Jin, C., Zheng, J., Wang, Y., Xu, Q., 2008. The stratigraphic distribution and zoogeography of the Early Pleistocene mammalian fauna from South China. Acta Anthropol. Sin. 27(4), 304–317.
Jin, C., Pan, W., Zhang, Y., Cai, Y., Xu, Q., Tang, Z., Wang, W., Wang, Y., Liu, J., Qin, D., Edwards, R.L., Cheng, H., 2009. The *Homo sapiens* cave hominin site of Mulan mountain, Jiangzhou district, Chongzuo, Guangxi with emphasis on its age. Chin. Sci. Bull. 54, 3848–3856.
Jin, C., Wang, Y., Deng, C., Harrison, T., Qin, D., Pan, W., Zhang, Y., Zhu, M., Yan, Y., 2014. Chronological sequence of the early Pleistocene *Gigantopithecus* faunas from cave sites in the Chongzuo, Zuojiang river area, south China. Quat. Int. 354, 4–14.
Kahlke, H.D., Hu, C., 1961. On the Complex of the *Stegodon-Ailuropoda*-Fauna of Southern China and the Chronological Position of *Gigantopithecus Blacki* v. koenigswald. Vertebr. PalAsiat. 02, 3–28.
Li, Y.-y., Pei, S.-w., Tong, H.-w., Yang, X.-x., Cai, Y.-j., Liu, W., Wu, X.-j., 2013. A Preliminary Report on the 2011 Excavation at Houbeishan Fuyan Cave, Daoxian, Hunan Province. Acta Anthropol. Sin. 32, 133–143.
Liang, H., Liao, W., Yao, Y., Bae, C.J., Wang, W., 2020a. A late Middle Pleistocene mammalian fauna recovered in northeast Guangxi, southern China: Implications for regional biogeography. Quat. Int. 563, 29–37.
Liang, H., 2020b. Middle Pleistocene Orangutan Fossil from Ganxian Cave, Tiandong County, Guangxi, South China and its Significance of Evolution. Thesis of Guilin University of Technology.

Lisiecki, L.E., Raymo, M.E., 2005. A Pliocene-Pleistocene stack of 57 globally distributed benthic $\delta^{18}O$ records. Paleoceanography 20, 1–17.

Liu, W., Jin, C.-Z., Zhang, Y.-Q., Cai, Y.-J., Xing, S., Wu, X.-J., Cheng, H., Edwards, R.L., Pan, W.-S., Qin, D.-G., 2010. Human remains from Zhirendong, south China, and modern human emergence in east Asia. Proc. Natl. Acad. Sci. 107, 19201–19206.

Liu, W., Martinón-Torres, M., Cai, Y.-j., Xing, S., Tong, H.-w., Pei, S.-w., Sier, M.J., Wu, X.-h., Edwards, R.L., Cheng, H., 2015. The earliest unequivocally modern humans in southern China. Nature 526, 696–699.

Long X., 1994. The chorography of Pubei. Guangxi People's Publishing house, Nanning.

Long, V.T., de Vos, J., Ciochon, R.S., 1996. The fossil mammal fauna of the Lang Trang caves, Vietnam, compared with Southeast Asian fossil and recent mammal faunas: The geographical implications. Bulletin of the Indo-Pacific Prehistory Association 14, 101–109.

Louys, J., Roberts, P., 2020. Environmental drivers of megafauna and hominin extinction in Southeast Asia. Nature 586, 1–5.

Lu, C., 2010. Late Pleistocene mammalian fauna from Yangjiapuo Cave, Jianshi, Hubei, in: Dong Wei (Ed), Proceedings of the Twelfth Annual Meeting of the Chinese Society of Vertebrate Paleontology. China Ocean Press, Beijing, pp. 97–120.

Ma, J., Wang, Y., Jin, C., Yan, Y., Qu, Y., Hu, Y., 2017. Isotopic evidence of foraging ecology of Asian elephant (*Elephas maximus*) in South China during the late Pleistocene. Quat. Int. 443, 160–167.

Martinón-Torres, M., Cai, Y., Tong, H., Pei, S., Xing, S., Bermudez de Castro, J.M., Wu, X., Liu, W., 2021. On the misidentification and unreliable context of the new "human teeth" from Fuyan Cave (China). Proc. Natl Acad. Sci. 118, e2102961118.

Matthew, W., Granger, W., 1923. New fossil mammals from the Pliocene of Szechuan, China. Bull. Am. Mus. Nat. Hist. 48, 563–598.

Nelson, S.V., 2014. The paleoecology of early Pleistocene *Gigantopithecus blacki* inferred from isotopic analyses. Am. J. Phys. Anthropol. 155, 571–578.

Norton, C.J., Jin, C., Wang, Y., Zhang, Y., 2010. Rethinking the Paleartic-oriental biogeographic boundary in Quaternary China, in: Norton, C. J., Braun, D. R. (Eds)., Asian paleoanthropology: From Africa to China and beyond. Vertebrate Paleobiology and Paleoanthropology, Dordrecht: Springer Netherlands, pp. 81–100.

Pan, Y., 2021. An α-taxonomy study of the late Middle Pleistocene mammalian fauna from the Yixiantian Cave, Chongzuo, Guangxi Zhuang Autonomous Region. Thesis of University of Chinese Academy of Sciences.

Patte, E., 1928. Comparaison des faunes de mammifères de Langson (Tonkin) et du SE Tchouen. Bull. Soc. Géol. Fr. 28, 55–63.

Pei, W.Z., 1935. Fossil mammals from the Kwangsi caves. Bulletin of the Geological Society of China 14(03), 413–425.

Pei, W., 1938. Le rôle des animaux et des causes naturelles dans la cassure des os. Palaeontologica Sinica 118, 1–61.

Pei, W., 1980. *Ailuropoda-Stegodon* Fauna. Journal of Guizhou Normal University (Social Science) 1, 3–9.

Pei, W., 1987. Carnivora, Proboscidea and Rodentia from Liucheng *Gigantopithecus* Cave and other caves in Guangxi. Memoirs of Institute of Vertebrate Palaeontology and

Palaeoanthropology, Academia Sinica 18, 1–134.
Pope, G.G., Frayer, D.W., Liangchareon, M., Kulasing, P., Nakabanlang, S., 1981. Palaeoanthropological investigations of the Thai-American expeditions in Northern Thailand (1978-1980): An interim report. Asian Perspect. 21, 147–163.
Qiu, Z., 2006. Quaternary environmental changes and evolution of large mammals in North China. Vertebr. PalAsiat. 44(2), 109–132.
Rink, W.J., Wei, W., Bekken, D., Jones, H.L., 2008. Geochronology of *Ailuropoda–Stegodon* fauna and *Gigantopithecus* in Guangxi Province, southern China. Quat. Res. 69, 377–387.
Roth, V.L., Shoshani, J., 1988. Dental identification and age determination in *Elephas maximus*. J. Zool. 214, 567–588.
Shao, Q.-F., Pons-Branchu, E., Zhu, Q.-P., Wang, W., Valladas, H., Fontugne, M., 2017. High precision U/Th dating of the rock paintings at Mt. Huashan, Guangxi, southern China. Quat. Res. 88 (1), 1–13.
Shao, Q.-F., Li, C.-H., Huang, M.-J., Liao, Z.-B., Arps, J., Huang, C.-Y., Chou, Y.-C., Kong, X.-G., 2019. Interactive programs of MC-ICPMS data processing for 230Th/U Geochronology. Quat. Geochronol. 51, 43–52.
Smith, H.E., Price, G.J., Duval, M., Westaway, K., Zaim, J., Rizal, Y., Aswan, Puspaningrum, M.R., Trihascaryo, A., Stewart, M., Louys, J., 2021. Taxonomy, taphonomy and chronology of the Pleistocene faunal assemblage at Ngalau Gupin cave, Sumatra. Quat. Int. 603, 40–63.
Stacklyn, S., Wang, Y., Jin, C., Wang, Y., Sun, F., Zhang, C., Jiang, S., Deng, T., 2017. Carbon and oxygen isotopic evidence for diets, environments and niche differentiation of early Pleistocene pandas and associated mammals in South China. Palaeogeogr., Palaeoclim., Palaeoecol. 468, 351–361.
Stewart, J.R., 2009. The evolutionary consequence of the individualistic response to climate change. J. Evol. Biol. 22, 2363–2375.
Storm, P., Aziz, F., de Vos, J., Kosasih, D., Baskoro, S., van den Hoek Ostende, L.W., 2005. Late Pleistocene *Homo sapiens* in a tropical rainforest fauna in east Java. J. Hum. Evol. 49, 536–545.
Storm, P., de Vos, J.D., 2006. Rediscovery of the late Pleistocene Punung hominin sites and the discovery of a new site Gunung Dawung in east Java. Senckenberg Lethaea 86(2), 121–131.
Sun, L., Wang, Y., Liu, C., Zuo, T., Ge, J., Zhu, M., Jin, C., Deng, C., Zhu, R., 2013. Magnetic polarity chronology sequence of *Gigantopithecus* fauna in Chongzuo area, Guangxi. The Chinese Geophysics 2013.
Sun, F., Wang, Y., Wang, Y., Jin, C., Deng, T., Burt, W., 2019. Paleoecology of Pleistocene mammals and paleoclimatic change in South China: Evidence from stable carbon and oxygen isotopes. Palaeogeogr. Palaeoclim. Palaeoecol. 524, 1–12.
Sun, J.-J., Zhang, B., Chen, X., Deng, L., Wen, J., Tong, H.-w., 2021. New fossils of Late Pleistocene *Sus scrofa* from Yangjiawan Cave 2, Jiangxi, China. Vertebr. PalAsiat. 59(1), 64–80.
Sun, X.F., Wen, S.Q., Lu, C.Q., Zhou, B.Y., Curnoe, D., Lu, H.Y., Li, H.C., Wang, W., Cheng, H., Yi, S.W., Jia, X., Du, P.X., Xu, X.H., Lu, Y.M., Lu, Y., Zheng, H.X., Zhang, H., Sun, C., Wei, L.H., Han, F., Huang, J., Edwards, R.L., Jin, L., Li, H., 2021. Ancient DNA and multimethod dating confirm the late arrival of anatomically modern humans in southern China. Proc. Natl. Acad. Sci. 118(8), 2019158118.
Suraprasit, K., Bocherens, H., Chaimanee, Y., Panha, S., Jaeger, J.-J., 2018. Late Middle Pleistocene

ecology and climate in Northeastern Thailand inferred from the stable isotope analysis of Khok Sung herbivore tooth enamel and the land mammal cenogram. Quat. Sci. Rev. 193, 24–42.

Suraprasit, K., Jaeger, J.-J., Chaimanee, Y., Sutcharit, C., 2020. Taxonomic reassessment of large mammals from the Pleistocene Homo-bearing site of Tham Wiman Nakin (northeast Thailand): Relevance for faunal patterns in mainland southeast Asia. Quat. Int. 603, 90–112.

Swindler, D.R., 2002. Primate Dentition. Cambridge University Press, Cambridge.

Takai, M., Zhang, Y., Kono, R.T., Jin, C., 2014. Changes in the composition of the Pleistocene primate fauna in southern China. Quat. Int. 354, 75–85.

Tasumi, M., 1964. The cheek teeth of a young Indian elephant. Mammalia 28(3), 381–396.

Tong, H.-w., 2001. Rhinocerotids in China - Systematics and material analysis. Geobios 34, 585–591.

Tong, H.-w., 2005. *Hystrix subcristata* (Mammalia, Rodentia) from Tianyuan Cave, a human fossil site newly discovered near Zhoukoudian (Choukoutien). Vertebr. PalAsiat. 43(2), 135–150.

Tong, H.-w., Deng, L., Chen, X., Zhang, B., Wen, J., 2018. Late Pleistocene proboscideans from Yangjiawan caves in Pingxiang of Jiangxi, with discussions on the *Stegodon orientalis-Elephas maximus* assemblage. Vertebr. PalAsiat. 56(4), 306–326.

Tong, H.-w., Zhang, B., Wu, X., Qu, S., 2019. Mammalian fossils from the Middle Pleistocene human site of Bailongdong in Yunxi, Hubei. Acta Anthropol. Sin. 38, 613–640.

Tougard, C., 2001. Biogeography and migration routes of large mammal faunas in South-East Asia during the Late Middle Pleistocene: Focus on the fossil and extant faunas from Thailand. Palaeogeogr., Palaeoclim., Palaeoeco. 168, 337–358.

Turvey, S.T., Tong, H., Stuart, A.J., Lister, A.M., 2013. Holocene survival of Late Pleistocene megafauna in China: A critical review of the evidence. Quat. Sci. Rev. 76, 156–166.

Wang, W., 2005 Early Pleistocene Hominoid Fossil Assemblage from Mohui Cave, Tiandong County, Guangxi, South China and its Significance of Early Human Evolution. Thesis of China University of Geosciences.

Wang, W., Potts, R., Baoyin, Y., Huang, W., Cheng, H., Edwards, R.L., Ditchfield, P., 2007. Sequence of mammalian fossils, including hominoid teeth, from the Bubing Basin caves, South China. J. Hum. Evol. 52, 370–379.

Wang, Y., Cheng, H., Lawrence Edwards, R., Kong, X. Shao, X., Chen, S., Wu, J., Jiang, X. Wang, X., An, Z., 2008. Millennial- and orbital-scale changes in the East Asian monsoon over the past 224,000 years. Nature 451, 1090–1093.

Wang, W., Liao, W., Li, D., Tian, F., 2014. Early Pleistocene large-mammal fauna associated with *Gigantopithecus* at Mohui cave, Bubing basin, south China. Quat. Int. 354, 122–130.

Wang, X., Xu, C., Tong, H., 2015. Pleistocene *Bos* (*Bibos*) *gaurus* from Bailong Cave in Yunxi County, Hubei, China. Acta Anthropol. Sin. 34(3), 338–352.

Wang, Y., Qin D., Jin, C., 2017. New *Elephas* remains from the Zhiren Cave of Mulan Mountain, Chongzuo, Guangxi with discussion on Quaternary Proboscidean evolution in Southern China. Quat. Sci. 37(4), 853–859.

Weers, P.J. van, Zheng, S.H., 1998. Biometric analysis and taxonomic allocation of Pleistocene *Hystrix* specimens (Rodentia, porcupines) from China. Beaufortia. 48, 47–69.

Westaway, K.E., Morwood, M.J., Roberts, R.G., Rokus, A.D., Zhao, J.-x., Storm, P., Aziz, F., van den Bergh, G., Hadi, P., Jatmiko, de Vos, J., 2007. Age and biostratigraphic significance of the

Punung rainforest fauna East Java, Indonesia, and implications for *Pongo* and *Homo*. J. Hum. Evol. 53, 709–717.

Woo, J.K, 1959. Human fossils found in the Liukiang, Kwangsi, China. Paleovertebrata et Palaeoanthropologica, 1(3), 97–104.

Yan, Y., Wang, Y., Jin, C., Mead, J.I., 2014. New remains of rhinoceros (Rhinocerotidae, Perissodactyla) associated with *Gigantopithecus blacki* from the Early Pleistocene Yanliang cave, Fusui, South China. Quat. Int. 354, 110–121.

Zhang, Y., Jin, C., Cai, Y., Kono, R., Wang, W., Wang, Y., Zhu, M., Yan, Y., 2014. New 400–320 ka *Gigantopithecus blacki* remains from Hejiang cave, Chongzuo City, Guangxi, South China. Quat. Int. 354, 35–45.

Zhang, B., Chen, X., Tong, H.-W., 2018. Tooth remains of Late Pleistocene moschid and cervid (Artiodactyla, mammalia) from Yangjiawan and Fuyan Caves of southern China. Quat. Int. 490, 21–32.

Zhao, L.X., Wang, C.B., Jin, C.Z., Qin, D.G., Pan, W.S., 2009. Fossil orangutan-like hominoid teeth from late Pleistocene human site of Mulanshan cave in Chongzuo of Guangxi and implications on taxonomy and evolution of orangutan. Chin. Sci. Bull. 54, 2924–2930.

Zhao, L.X., Zhang, L.Z., 2013. New fossil evidence and diet analysis of *Gigantopithecus blacki* and its distribution and extinction in South China. Quat. Int. 286, 69–74.

Zheng, S., 1993. Quaternary Rodentia in Sichuan and Guizhou. China Science Publishing, Beijing.

Zheng, S., 2004. Jianshi Hominid Site. China Science Publishing, Beijing.

Zhou, M., 1957. The nature and comparation of Tertiary and Early Quaternary mammalian fauna in South China. Chinese Sci. Bull. 13, 394–400.

Zin-Maung-Maung-Thein, Takai, M., Tsubamoto, T., Thaung-Htike, Egi, N., Maung-Maung, 2008. A new species of *Dicerorhinus* (Rhinocerotidae) from the Plio-Pleistocene of Myanmar. Paleontology 51, 1419–1433.

Zong, G., 1987. Note on some mammalian fossils of Yanyuan, Sichuan. Vertebr. PalAsiat. 25(2), 137–145.